

**CHEMICAL DEGRADATION REVIEW**

**Cementitious Barriers Partnership**

**November 2009**

**CBP-TR-2009-002-C4, Rev. 0**

## **ACKNOWLEDGEMENTS**

This report was prepared for the United States Department of Energy in part under Contract No. DE-AC09-08SR22470 and is an account of work performed in part under that contract. This report was prepared in support of the Savannah River Nuclear Solutions Cooperative Research Agreement (CRADA) CR-08-001. Reference herein to any specific commercial product, process, or service by trademark, name, manufacturer, or otherwise does not necessarily constitute or imply endorsement, recommendation, or favoring of same by Savannah River Nuclear Solutions or by the United States Government or any agency thereof. The views and opinions of the authors expressed herein do not necessarily state or reflect those of the United States Government or any agency thereof.

**and**

This report is based in part on work supported by the United States Department of Energy under Cooperative Agreement Number DE-FC01-06EW07053 entitled “The Consortium for Risk Evaluation with Stakeholder Participation III” awarded to Vanderbilt University. The opinions, findings, conclusions, or recommendations expressed herein are those of the author(s) and do not necessarily represent the views of the Department of Energy or Vanderbilt University.

## **Disclaimer**

This work was prepared under an agreement with and funded by the U. S. Government. Neither the U.S. Government or its employees, nor any of its contractors, subcontractors or their employees, makes any express or implied: 1. warranty or assumes any legal liability for the accuracy, completeness, or for the use or results of such use of any information, product, or process disclosed; or 2. representation that such use or results of such use would not infringe privately owned rights; or 3. endorsement or recommendation of any specifically identified commercial product, process, or service. Any views and opinions of authors expressed in this work do not necessarily state or reflect those of the United States Government, or its contractors, or subcontractors, or subcontractors.

**Printed in the United States of America**

**United State Department of Energy  
Office of Environmental Management  
Washington, DC**

**This document is available on the CBP website: <http://cementbarriers.org/>**

**and**

**Savannah River National Laboratory website: <http://srnl.doe.gov>**

## **FOREWORD**

The Cementitious Barriers Partnership (CBP) Project is a multi-disciplinary, multi-institutional collaboration supported by the United States Department of Energy (US DOE) Office of Waste Processing. The objective of the CBP project is to develop a set of tools to improve understanding and prediction of the long-term structural, hydraulic, and chemical performance of cementitious barriers used in nuclear applications.

A multi-disciplinary partnership of federal, academic, private sector, and international expertise has been formed to accomplish the project objective. In addition to the US DOE, the CBP partners are the United States Nuclear Regulatory Commission (NRC), the National Institute of Standards and Technology (NIST), the Savannah River National Laboratory (SRNL), Vanderbilt University (VU) / Consortium for Risk Evaluation with Stakeholder Participation (CRESP), Energy Research Center of the Netherlands (ECN), and SIMCO Technologies, Inc.

The periods of cementitious performance being evaluated are >100 years for operating facilities and > 1000 years for waste management. The set of simulation tools and data developed under this project will be used to evaluate and predict the behavior of cementitious barriers used in near-surface engineered waste disposal systems, e.g., waste forms, containment structures, entombments, and environmental remediation, including decontamination and decommissioning (D&D)

activities. The simulation tools also will support analysis of structural concrete components of nuclear facilities (spent-fuel pools, dry spent-fuel storage units, and recycling facilities such as fuel fabrication, separations processes). Simulation parameters will be obtained from prior literature and will be experimentally measured under this project, as necessary, to demonstrate application of the simulation tools for three prototype applications (waste form in concrete vault, high-level waste tank grouting, and spent-fuel pool). Test methods and data needs to support use of the simulation tools for future applications will be defined.

The CBP project is a five-year effort focused on reducing the uncertainties of current methodologies for assessing cementitious barrier performance and increasing the consistency and transparency of the assessment process. The results of this project will enable improved risk-informed, performance-based decision-making and support several of the strategic initiatives in the DOE Office of Environmental Management Engineering & Technology Roadmap. Those strategic initiatives include 1) enhanced tank closure processes; 2) enhanced stabilization technologies; 3) advanced predictive capabilities; 4) enhanced remediation methods; 5) adapted technologies for site-specific and complex-wide D&D applications; 6) improved SNF storage, stabilization and disposal preparation; 7) enhanced storage, monitoring and stabilization systems; and 8) enhanced long-term performance evaluation and monitoring.

**Christine A. Langton, PhD.**  
**Savannah River National Laboratory**

**David S. Kosson, PhD.**  
**Vanderbilt University/CRESP**



## **CHEMICAL DEGRADATION REVIEW**

Eric Samson

Email: [esamson@simcotechnologies.com](mailto:esamson@simcotechnologies.com)  
SIMCO Technologies, Inc.  
Quebec City, Canada

Pierre Henocq

Email: [phenocq@simcotechnologies.com](mailto:phenocq@simcotechnologies.com)  
SIMCO Technologies, Inc.  
Quebec City, Canada

Jacques Marchand

Email: [jmarchand@simcotechnologies.com](mailto:jmarchand@simcotechnologies.com)  
SIMCO Technologies, Inc.  
Quebec City, Canada

November 2009

CBP-TR-2009-002-C4, Rev. 0



<b>CONTENTS</b>	<b>Page No.</b>
<b>LIST OF FIGURES .....</b>	<b>IV-viii</b>
<b>LIST OF TABLES.....</b>	<b>IV-ix</b>
<b>LIST OF ABBREVIATIONS AND ACRONYMS .....</b>	<b>IV-x</b>
<b>LIST OF SYMBOLS.....</b>	<b>IV-xi</b>
<b>ABSTRACT.....</b>	<b>IV-1</b>
<b>1.0 INTRODUCTION.....</b>	<b>IV-1</b>
<b>2.0 TRANSPORT MECHANISMS .....</b>	<b>IV-2</b>
<b>2.1 Ionic Transport.....</b>	<b>IV-2</b>
<b>2.2 Moisture Transport .....</b>	<b>IV-6</b>
<b>2.3 Diffusion Potential.....</b>	<b>IV-7</b>
<b>2.4 Temperature-Field Modeling .....</b>	<b>IV-8</b>
<b>3.0 CHLORIDE INGRESS AND CORROSION .....</b>	<b>IV-8</b>
<b>3.1 Chloride Interaction with Hydrated Cement Systems .....</b>	<b>IV-8</b>
<b>3.2 Binding Mechanisms.....</b>	<b>IV-9</b>
<b>3.3 Modeling Chloride Ingress.....</b>	<b>IV-11</b>
<b>3.4 Prediction of Corrosion Initiation .....</b>	<b>IV-12</b>
<b>4.0 CARBONATION .....</b>	<b>IV-12</b>
<b>4.1 Description of the Carbonation Process.....</b>	<b>IV-14</b>
<b>4.2 Carbonation Measurements.....</b>	<b>IV-16</b>
<b>4.3 Carbonation Models.....</b>	<b>IV-16</b>
<b>5.0 DECALCIFICATION .....</b>	<b>IV-17</b>
<b>5.1 Description of the Process.....</b>	<b>IV-18</b>
<b>5.2 Experiments and Methods.....</b>	<b>IV-19</b>
<b>5.3 Modeling the Decalcification Process .....</b>	<b>IV-22</b>
<b>6.0 SULFATE ATTACK .....</b>	<b>IV-23</b>
<b>6.1 Description of the Sulfate Attack Process .....</b>	<b>IV-25</b>
<b>6.2 Experiments and Methods.....</b>	<b>IV-29</b>
<b>6.3 External Sulfate Attack Modeling .....</b>	<b>IV-31</b>
<b>7.0 CONCLUSIONS .....</b>	<b>IV-33</b>
<b>8.0 REFERENCES.....</b>	<b>IV-34</b>

**LIST OF FIGURES**

**Page No.**

Figure 1.	Contributions of the Chloride Chemical and Physical Binding In A Cement System (from (Hosokawa 2006)).....	IV-10
Figure 2.	Predicted Total Chloride Profile in A 20-year-old Parking Structure Using the Model Presented in (Samson 2007), Compared to Measurements Performed on Two Cores. (The inserted graph illustrates the time-dependent boundary conditions over one year.).....	IV-13
Figure 3.	Chloride Content at Different Rebar Positions(The calculations correspond to the case presented in Figure 2).....	IV-13
Figure 4.	Relative Distribution of CO <sub>2</sub> (aq), HCO <sub>3</sub> <sup>-</sup> and CO <sub>3</sub> <sup>2-</sup> as a Function of pH at 25°C.....	IV-15
Figure 5.	Carbonation Depths (a) Measured with Phenolphthalein on Mortar Samples Exposed to a 50% RH 5% CO <sub>2</sub> Environment and (b) Plotted Against the Square Root of Time. (Data provided by SIMCO Technologies Inc.).....	IV-16
Figure 6.	Change of Ca <sup>2+</sup> Concentration as A Function of the Leaching Duration (a) and Depth of the Ca(OH) <sub>2</sub> Dissolved Front as A Function of the Square Root of the Leaching Period (b) (Haga 2005).....	IV-19
Figure 7.	Pore Size Distribution on Sound and Leached Samples (Haga 2005)).....	IV-20
Figure 8.	Cumulative Quantity of Dissolved Ca <sup>2+</sup> for SCM Mixtures (a) Blast-furnace Slag (BF) and (b) Silica Fume (SF) (Saito 2000)).....	IV-20
Figure 9.	(a) Relationship Between Pore Volume (PV/Vp) and Compressive Strength for Sound and Degraded Materials (Saito 2000) and (b) Variation of the Strength Loss in Relation to the Degradation Ratio Ad/At ( adapted from Carde 1996).....	IV-21
Figure 10.	Relationship Between [Ca] in the Solution and the Solid Content from Daimon et al. (Haga 2005, Daimon 1977).....	IV-22
Figure 11.	Simulations of Calcium Leaching (a) on Cement Paste (Maltais 2004) and (b) on Mortar (Yokozeki 2004).....	IV-24
Figure 12.	Expansions of Mortars Under Sodium Sulfate Attack as A Function of W/C: (a) (Naik 2006) and (b) (Lee 2005).....	IV-26
Figure 13.	Expansion of Mortars Under Sodium Sulfate Attack vs. C3A Content (a) %C3A type I > %C3A type V (Naik 2006) and (b) (Ouyang 1988).....	IV-27
Figure 14.	Expansions of Sandberg Prisms for Different Slag Contents (a) in Na <sub>2</sub> SO <sub>4</sub> Solution (1.5 % SO <sub>3</sub> ) and (b) in MgSO <sub>4</sub> Solution (1.5 % SO <sub>3</sub> ).....	IV-28
Figure 15.	Expansions of PLC Mortar Prisms Containing Fly Ash After Immersion in 4.4 % Sodium Sulfate Solution (Mulenga 2003).....	IV-30
Figure 16.	Sulfur Content Mapping (a) and Sulfur Profiles (b) for 0.6 W/C Ratio CSA Type 10 Cement Pastes Exposed for 3 Months to a 50 mmol/l Na <sub>2</sub> SO <sub>4</sub> Solution (Maltais 2004).....	IV-32

**LIST OF TABLES**

**Page No.**

Table 1. Solubility Constants of Portlandite and C-S-H (Maltais 2004, Berner 1992)..... IV-23

Table 2.  $D = M(\phi)$  Relationships Found in Literature ..... IV-23

Table 3. Solubility Constants of Solid Phases Involved During Sulfate Ingress in Hydrated  
Cement Systems (Maltais 2004)..... IV-33

**LIST OF ABBREVIATIONS AND ACRONYMS**

ADE	Advective-Dispersive Equation or Advective-Diffusive Equation
ASR	Alcali-Silica Reaction
DEF	Delayed Ettringite Formation
FHWA	Federal Highway Administration
HMW	Harvies, Moller and Weare implementation of Pitzer's ionic interaction model
LEA	Local Equilibrium Assumption
opc	ordinary Portland cement
REV	Representative Elementary Volume
SIA	Sequential Iterative Approach
SNIA	Sequential Non Iterative Approach

## LIST OF SYMBOLS

$a$	Hydration parameter (see $H(t)$ )
$A$	Parameter in the exponential water diffusivity expression $D_w = Ae^{Bw}$
$B$	Parameter in the exponential water diffusivity expression $D_w = Ae^{Bw}$
$c_i$	Concentration of species $i$ in solution at the pore scale
$C_i$	Concentration of species $i$ in solution averaged over a REV
$C_p$	Heat capacity
$D_i^o$	Freewater diffusion coefficient of species $i$ (self-diffusion coefficient)
$D_i$	Diffusion coefficient of species $i$ in solution at the material scale
$D_{app}$	Chloride apparent diffusion coefficient
$D_h$	Water diffusivity as a function of relative humidity
$D_w$	Water diffusivity as a function of water content
$F$	Faraday constant
$G(T)$	Effect of temperature on diffusion coefficients
$H(t)$	Effect of hydration on diffusion coefficients
$I$	Ionic strength
$j_i$	Flux of species $i$
$k$	Thermal conductivity
$K$	Intrinsic permeability
$k_{ri}$	Relative permeability of fluid $i$
$M(\phi)$	Function relating changes in porosity to changes in transport properties
$N$	Number of species in solution
$p$	pressure
$r_i$	Source/sink term for the homogeneous reaction at the pore scale
$R$	Ideal gas constant
$R_i$	Source/sink term for the homogeneous reaction averaged over a REV
$S_i$	Saturation level of fluid phase $i$
$S(w)$	Effect of water content on diffusion coefficients
$S(h)$	Effect of relative humidity on diffusion coefficients
$t$	time
$T$	Temperature
$U$	Activation energy
$v_i$	Velocity of fluid $i$ at the pore scale
$V_i$	Velocity of fluid $i$ averaged over a REV
$V_p$	Paste volume in a cementitious material mixture
$w$	Water content
$x, y, z$	Position
$\alpha$	Rate parameter in the hydration function $H(t)$
$\alpha$	Parameter in the water diffusivity function $D(h)$
$\beta$	Parameter in the water diffusivity function $D(h)$
$\varepsilon$	Permittivity
$\phi$	Porosity
$\gamma$	Parameter in the water diffusivity function $D(h)$

**LIST OF SYMBOLS (contd)**

$\gamma_i$	Chemical activity coefficient of species $i$
$\eta$	Dynamic viscosity
$\mu_i$	Electrochemical potential
$\mu_{l \rightarrow v}, \mu_{v \rightarrow l}$	Water vaporization/condensation terms
$\theta^s$	Solid phase content
$\rho_i$	Density of phase $i$
$\tau$	Tortuosity
$\psi$	Diffusion potential at the pore scale
$\Psi$	Diffusion potential averaged over a REV

# CHEMICAL DEGRADATION REVIEW

Eric Samson  
Pierre Henocq  
Jacques Marchand  
SIMCO Technologies, Inc.  
Quebec City, Canada

---

## ABSTRACT

This report reviews the most common mechanisms associated with the chemical degradation of cementitious materials. The review focuses on cases where the chemical degradation of the materials is triggered by the exchange of ionic species at the material/environment interface. In some cases, ionic species are leached out of the material while in other cases, external contaminants enter the material and affect the microstructure. Many situations involve simultaneous species ingress and leaching.

Since the transport of species is prominently involved in the chemical degradation of cementitious materials, the various mechanisms affecting the movement of ions in the pore solution of cementitious materials was first reviewed. Part of the review is dedicated to moisture transport. A more detailed report on this topic can be found in Chapter 2d.

Following this, common chemical degradation mechanisms were reviewed, namely chloride ingress and corrosion, carbonation, decalcification due to the leaching of hydroxide and calcium and external sulfate attack.

As mentioned earlier, only cases involving the exchange of ions at the material/environment interface were considered. “Internal” degradation mechanisms such as delayed ettringite formation (DEF) and alkali-silica reaction (ASR) were left aside. Although they are commonly observed on many existing structures, they can be avoided with proper material selection and concrete practice.

Various types of cementitious materials were described in the paper reviewed. The papers dealing with chloride ingress featured mostly mortar and concrete mixtures, while the carbonation studies were primarily made on hydrated cement pastes and mortars. In the case of external sulfate attack and decalcification, the papers reviewed in this chapter were mostly based on hydrated cement pastes, which make characterization easier due to the absence of aggregates. No studies dedicated specifically to wastefirms were reviewed.

---

## 1.0 INTRODUCTION

While interacting with its service environment, concrete and other cementitious materials often undergo significant alterations that often have adverse consequences on their engineering properties. As a result, the durability of hydrated cement systems and their constituent phases has been studied

closely by scientists and engineers. The alteration to microstructure occurs mostly following ionic exchanges between the hydrated cement paste and the environment. The exchanges affect the equilibrium between the pore solution of cementitious materials and the solid phases of the paste, resulting in dissolution and/or precipitation of minerals.

Since the transport of species is prominently involved in the chemical degradation of cementitious materials, the various mechanisms affecting the movement of ions in the pore solution of cementitious materials were reviewed. The basic principles of gas transport are also outlined. A section of the review is also dedicated to moisture transport. However, a more detailed report on this topic can be found in the chapter dedicated to hydraulic properties.

Then, different chemical degradation phenomena were reviewed. Microstructural alterations resulting from exposure to chlorides and carbon dioxide are discussed. Sulfate attack from external sources is described including processes resulting in the formation of ettringite and thaumasite. Finally, the decalcification of hydrated cement pastes resulting from the leaching of calcium and hydroxide in the external environment is discussed. Some chemical degradation phenomena ultimately lead to physical damage on the material. The mechanical aspects were reviewed in the chapter dedicated to the mechanical damage review.

The review only focused on degradation cases involving the exchange of ions at the material/environment interface. “Internal” degradation mechanisms such as delayed ettringite formation (DEF) and alkali-silica reaction (ASR) were left aside. DEF affects structures that exhibited internal temperature above 70°C during the hydration process, resulting in a deleterious dissolution/precipitation sequence for ettringite. ASR is concerned with the formation of a gel around reactive aggregates that causes tension and ultimately cracks in the concrete. Although these two mechanisms are commonly observed on many existing structures, they can be avoided with proper material selection and concrete practice.

The paper reviewed showed a large range of material types. The papers dealing with chloride ingress featured mostly mortar and concrete mixtures, while the carbonation studies were primarily made

on hydrated cement pastes and mortars. In the case of external sulfate attack and decalcification, the papers reviewed in this chapter were mostly based on hydrated cement pastes, which make characterization easier due to the absence of aggregates. No studies dedicated specifically to wastefoms were reviewed.

## 2.0 TRANSPORT MECHANISMS

### 2.1 Ionic Transport

The development of ionic transport models in cementitious materials has initially been motivated by concerns over the premature degradation of concrete structures exposed to chloride-laden environments. Early models were typically limited to simplified equations describing the diffusion of a single ion (e.g., chloride) in saturated concrete. These simple models were gradually improved to account for the complexity of ionic transport in unsaturated systems. Multi-ionic models that consider not only diffusion but other transport mechanisms, such as water movement under the effect of humidity gradients, were proposed and tested.

The description of transport phenomena is usually performed by writing the mass conservation equations at the pore level. The equations are then averaged over a Representative Elementary Volume (REV) of the material. By solving the averaged mass transport equations, one can therefore perform simulations at the scale of the concrete element.

At the pore scale, it is typically assumed that ions can be transported by a combination of two phenomena: an electrochemical potential gradient and the advection caused by a flow of the aqueous solution (Bockris 1970, Helfferich 1961):

$$\mathbf{j}_i = - \underbrace{\frac{D_i^o}{RT} c_i \text{grad}(\mu_i)}_{\text{electrochemical}} + \underbrace{c_i \mathbf{v}}_{\text{advection}} \quad (1)$$

where:  $c_i$  is the concentration of ionic species  $i$ ,  $D_i^o$  is the diffusion coefficient in free water,  $\mu_i$  is the electrochemical potential,  $R$  is the ideal gas constant,  $T$  is the temperature and  $\mathbf{v}$  is the velocity of the liquid phase.

The electrochemical potential  $\mu_i$  is defined as:

$$\mu_i = \mu_i^o + RT \ln(\gamma_i c_i) + z_i F \psi \quad (2)$$

where:  $\mu_i^o$  is a reference level,  $\gamma_i$  is the chemical activity coefficient,  $z_i$  is the valence number of the ionic species,  $F$  is the Faraday constant and  $\psi$  is the diffusion potential.

Substituting Equation (1) in (2) yields (Samson 2007):

$$\begin{aligned} \mathbf{j}_i = & -D_i^o \text{grad}(c_i) - \frac{D_i^o z_i F}{RT} c_i \text{grad}(\psi) \\ & - D_i^o c_i \text{grad}(\ln \gamma_i) \\ & - \frac{D_i^o c_i \text{grad}(\ln \gamma_i)}{T} \text{grad}(T) + c_i \mathbf{v} \end{aligned} \quad (3)$$

Each term on the right-hand side of Eq. (3) corresponds to a different mechanism. The first term, often called the diffusion term or Fick's law, describes the movement of ionic species under the effect of a concentration gradient.

The second term involving the diffusion potential is responsible for maintaining the pore solution electroneutrality by slightly altering the velocity of individual species. The diffusion potential thus couples each individual flux equation (Sten-Knudsen 2002).

The chemical activity term is essentially a correction to the flux when the ionic strength of the pore solution is high. The chemical activity term in Equations (2) and (3) can be estimated using an equation that relates the chemical activity coefficient  $\gamma_i$  to the concentrations in solution. Classical electrochemical

models like the Debye-Hückel or extended Debye-Hückel relationship are valid for weak electrolytes for which the ionic strength is on the order of 100 mmol/L, while the Davies correction can be used to describe the behavior of more concentrated solutions, i.e., with ionic strengths up to 300 mmol/L (Pankow 1994). Pore solutions extracted from hydrated cement systems are more in the 300 mmol/L (Hidalgo 2001) to 900 mmol/L range (Reardon 1992). As reported in (Zemaitis 1986), many models were developed to estimate the activity coefficients for highly concentrated solutions. One of the most commonly used approach is the implementation of Pitzer's ionic interaction model proposed by Harvie, Moller and Weare (Harvie 1984). Pitzer's model was used by Reardon (Reardon 1990) to model the hydrated paste/solution chemical equilibrium.

The next term in Equation (3), which involves temperature, is called the Soret effect. It describes the influence of a temperature gradient on the ionic flux.

The constitutive Equation (3) can be simplified in some specific cases. For instance, the Soret effect term (i.e., the fourth term in the equation) which describes the influence of temperature gradient on ionic flux, can be neglected for isothermal cases. In saturated materials, the term associated with the fluid velocity is most of the time neglected since pressure gradients to which structures are usually exposed are too weak to induce a flow given the low permeability of concretes.

To get the complete transport equation, the constitutive Equation (3) is substituted in the mass conservation relationship (Bear 1991):

$$\frac{\partial c_i}{\partial t} + \text{div}(\mathbf{j}_i) + r_i = 0 \quad (4)$$

where:  $r_i$  is the reaction rate term accounting for complexation in the solution. The complexation reactions are assumed to take place solely within the aqueous phase. The formation of  $\text{CaOH}^+$  is an example

of complexation reaction:  $\text{Ca}^{2+} + \text{OH}^- \leftrightarrow \text{CaOH}^+$ . At the pore scale, the other types of chemical reactions, i.e., dissolution/precipitation and surface adsorption, could be modeled by exchange terms at the aqueous/solid interface.

Combining Equations (3) and (4) gives the complete ionic transport equation in the aqueous phase at the pore scale:

$$\begin{aligned} \frac{\partial c_i}{\partial t} - \text{div} \left( D_i^o \text{grad}(c_i) \right. \\ \left. + \frac{D_i^o z_i F}{RT} c_i \text{grad}(\psi) + D_i^o c_i \text{grad}(\ln \gamma_i) \right) \\ \left. + \frac{D_i^o c_i \text{grad}(\ln \gamma_i)}{T} \text{grad}(T) - c_i \mathbf{v} \right) + r_i = 0 \end{aligned} \quad (5)$$

However, modeling transport of ions at the pore scale is currently a very difficult task. One has to have some 3-D representation of the entire porous network. The computational resources required to conduct these calculations are large but obtainable on modern parallel computers. To circumvent this difficulty, and to make the calculation more tractable, pore scale equations can be averaged over the scale of the material using a mathematical procedure called homogenization. The general application of the method can be found in (Bear 1991, Hassanizadeh 1979). The technique was specifically applied to cementitious materials in (Samson 2005). It should be noted that (Johannesson 2003) developed an ionic transport model on the basis of mixture theory and obtained similar results. In the homogenization (or averaging) technique, equations are integrated over the Representative Elementary Volume (REV) to lead to the equations at the scale of the material. The averaged form of Equation (5) is (Samson 2007):

$$\begin{aligned} \frac{\partial(\theta_s C_i^s)}{\partial t} + \frac{\partial(w C_i)}{\partial t} \\ - \text{div} \left( D_i w \text{grad}(C_i) + \frac{D_i z_i F}{RT} w C_i \text{grad}(\Psi) \right. \\ \left. + D_i w C_i \text{grad}(\ln \gamma_i) \right) \\ \left. + \frac{D_i C_i \text{grad}(\ln \gamma_i)}{T} w \text{grad}(T) - C_i \mathbf{V} \right) + w R_i = 0 \end{aligned} \quad (6)$$

where: the uppercase parameters represent the average of the corresponding quantity in Equation (5). The averaging process introduces the volumetric water content  $w$  in the mass transport equation. Also, a term involving the solid phase fraction  $\theta_s$  and the content of the ionic species  $i$  bound to the solid matrix,  $C_i^s$ , is now part of the relationship. This term is used to model chemical reactions between the pore solution and the hydrated cement paste. More details on the subject will be given in the following sections. On the contrary, the term  $R_i$  dedicated to homogeneous chemical reactions is in most cases neglected<sup>1</sup> in the papers reviewed for this report.

The parameter  $D_i$  in Equation (6) is the diffusion coefficient at the macroscopic level, which can be related to  $D_i^o$  by the expression:

$$D_i = \tau D_i^o \quad (7)$$

where:  $\tau$  is the tortuosity of the aqueous phase, a purely geometrical factor accounting for the complexity of the porous network.

Many authors have relied on this definition (Bear 1991, Samson 2007, Simunek 1994). Other authors (Emmanuel 2005, Zalc 2004) elected to work instead with the following definition:

$$D_i = \frac{D_i^o}{\tau} \quad (8)$$

---

<sup>1</sup> The situation is different in groundwater transport, where the homogeneous reactions are an important part of the pollutant movement process (see for instance (MacQuarrie 2005)).

Several factors can affect the diffusion coefficient such as the degree of saturation of the material, the ambient temperature, and any modification to the pore structure of the material (either induced by continuing hydration of chemical reactions). As proposed by Saetta et al. (Saetta 1993), the different factors can be expressed as separate functions such as:

$$D_i = \tau D_i^o \times S(w) \times G(T) \times H(t) \times M(\phi) \quad (9)$$

The function  $S(w)$  models the effect of the degree of saturation on the diffusion process. Few saturation models have been developed specifically for cement-based materials. Samson and Marchand (Samson 2007) used a relationship derived by Quirk and Millington for transport in groundwater:

$$S(w) = \frac{w^{7/3}}{\phi_o^{7/3}} \quad (10)$$

where:  $\phi_o$  is the initial porosity of the material.

In the approach developed by Saetta et al. (Saetta 1993), the function  $S$  is based on the relative humidity inside the material:

$$S(h) = \left( 1 + \frac{(1-h)^4}{(1-h_c)^4} \right)^{-1} \quad (11)$$

where:  $h_c$  is the critical humidity threshold at which the diffusion coefficient loses half its value.

The effect of temperature has traditionally been considered using an exponential relationship that features the activation energy (Saetta 1993):

$$G(T) = \exp \left[ \frac{U}{R} \left( \frac{1}{T_o} - \frac{1}{T} \right) \right] \quad (12)$$

where:  $U$  is the activation energy of the diffusion process and  $T_o$  is a reference temperature, usually around 25°C.

Recently, Samson et al. (Samson 2007) derived an expression that was found to properly describe the effect of temperature on the transport of ions in different materials:

$$G(T) = e^{0.028(T-T^o)} \quad (13)$$

Similarly, different relationships have been developed to model the effect of hydration on diffusion. Some are listed here:

$$H(t) = \begin{cases} a + (1-a) \left( \frac{t^{ref}}{t} \right)^{1/2} & (14) \\ \left( \frac{t^{ref}}{t} \right)^m & \text{(Thomas 1999) } (15) \\ \frac{a}{1 + (a-1)e^{-\alpha(t-t^{ref})}} & \text{(Samson 2007) } (16) \end{cases}$$

All these relationships have their maximum value early in the life of the material and decrease as the hydration process proceed. In most cases,  $t^{ref}$  is taken as 28 days. The relationships presented in references (Saetta 1993, Samson 2007) converge to a as  $t \rightarrow \infty$ , whereas the one in reference (Thomas 1999) decreases with time. The influence of continuous hydration on the transport properties of concrete can be particularly significant for mixtures prepared with supplementary cementing materials such as fly ash for which the low hydration rate means that transport properties a poor at early ages but decrease slowly over the years to yield high-performance materials.

As previously mentioned, chemical reactions can locally modify the pore structure of concrete and its transport properties. For instance, the formation of new phases can lead to a reduction of the material's porosity and contribute to reduce its transport properties. Likewise, the dissolution of existing phases can open the pore space and increase the diffusion coefficient. A modified version of the Kozeny-Carman relationship is often used in groundwater transport to calculate the correction factor  $M(\phi)$  that accounts for the effect of chemical alteration on the diffusion mechanism:

$$M(\phi) = \left( \frac{\phi}{\phi_o} \right)^3 \left( \frac{1-\phi_o}{1-\phi} \right)^2 \quad (17)$$

Relationships specifically devoted to cement-based materials have not been a major research topic. The following relationship was proposed recently (Samson 2006):

$$M(\phi) = \left( \frac{e^{4.3\phi/V_p}}{e^{4.3\phi_0/V_p}} \right) \quad (18)$$

where:  $V_p$  is the paste volume of the material.

In order to solve the general ionic transport Equation (6), other relationships are needed to evaluate the temperature, water content and diffusion potential fields. These points are described in the following sections.

The basic principles of ionic transport can be applied to gas transport. However, since the gas molecules do not bear electrical charges, the term associated with electrical coupling and chemical activity in Equation (6) are dropped. Also, the water content is replaced by the gas content. The interaction term in this case can account for the adsorption of gas on the pore walls of the material and on the dissolution of gas in the pore solution. These aspects are discussed in the section dedicated to carbonation.

## 2.2 Moisture Transport

Two main approaches have been used to model moisture movement in hydrated cement systems. The first one is based on a thorough description of all the phases involved in the process: liquid (aqueous solution), water vapor and dry air. Multiple mass conservation equations are invoked to obtain a description of the global moisture fields. The second approach can be derived from the first one under simplifying assumptions. It usually leads to the single equation (called the Richards' equation), which allows the water content field to be evaluated. Both approaches are reviewed in the following paragraphs. A more detailed literature review on moisture transport mechanisms in the hydraulic properties report.

Mainguy et al. (Mainguy 2001) relied on the multiphase approach to describe moisture movement under isothermal conditions. The mass balance equations for the three phases (liquid water ( $l$ ), dry air ( $a$ ) and water vapor ( $v$ )) that can be present in partially saturated concrete are given as:

### Liquid

$$\frac{\partial}{\partial t} (\phi \rho_l S_l) = -\text{div}(\phi S_l \rho_l \mathbf{v}_l) - \mu_{l \rightarrow v} \quad (19)$$

### Water Vapor

$$\frac{\partial}{\partial t} (\phi \rho_v (1 - S_l)) = -\text{div}(\phi (1 - S_l) \rho_v \mathbf{v}_v) + \mu_{l \rightarrow v} \quad (20)$$

### Dry Air

$$\frac{\partial}{\partial t} (\phi \rho_a (1 - S_l)) = -\text{div}(\phi (1 - S_l) \rho_a \mathbf{v}_a) \quad (21)$$

where:  $\phi$  is the porosity,  $\rho_i$  is the density of phase  $i$ ,  $S_l$  is the liquid water saturation,  $\mathbf{v}_i$  is the velocity of constituent  $i$ , and  $\mu_{l \rightarrow v}$  is the rate of liquid water vaporization.

The liquid phase velocity is given by the Darcy state law:

$$\phi \mathbf{v}_i = -\frac{K}{\eta_i} k_{ri}(S_l) \text{grad}(p_i) \quad (22)$$

where:  $K$  is the intrinsic permeability of the porous material,  $\eta_i$  is the dynamic viscosity of phase  $i$ ,  $k_{ri}(S_l)$  is the relative permeability and  $p_i$  is the pressure.

The dry air and vapor phases state law is given by Fick's relationship, expressed as:

$$\phi_g \rho_j \mathbf{v}_j = \phi_g \rho_j \mathbf{v}_g - \rho_j \frac{D}{C_j} f(S_l, \phi) \text{grad}(C_j) \quad (23)$$

where:  $\mathbf{v}_g$  is the gas molar-averaged velocity satisfying Darcy's law,  $D$  is the diffusion coefficient of water vapor or dry air in wet air,  $f$  is the resistance factor accounting for both the tortuosity effect and the reduction of space offered to the diffusion of gaseous constituents, and  $C_j$  is the ratio  $P_j/P_g$  with  $j = a$  or  $v$  (Degiovanni 1987).

Similar models were developed by Selih (Selih 1996) and Gawin (Gawin 2006). The model developed by Mainguy et al. (Mainguy 2001), has been found to properly reproduce isothermal drying test results. However, this approach has not been coupled with ionic transport models dedicated to cementitious materials.

Instead, a simplified approach is often selected to describe the variation in water content within cement-based materials. One of the main differences between two approaches is the assumption that gas pressure is uniform over the material and is equal to atmospheric pressure. Under this hypothesis, it has been shown (Samson 2005, Whitaker 1998) that the water content can be evaluated on the basis of Richards' equation:

$$\frac{\partial w}{\partial t} - \text{div}(D_w \text{grad}(w)) = 0 \quad (24)$$

where:  $w$  is the volumetric water content and  $D_w$  is the nonlinear water diffusivity parameter.

Using this approach, the velocity of the fluid phase appearing in Equation (6) is given by:

$$\mathbf{V} = -D_w \text{grad}(w) \quad (25)$$

It is commonly accepted that  $D_w$  follows an exponential relationship (Hall 1994):  $D_w = A \exp(Bw)$ , where  $B$  is positive. Instead of using the water content as a state variable, other authors have elected to model the relative humidity field  $h$ , under the assumption that the driving force can be expressed as:  $\mathbf{V} = -D_h \text{grad}(h)$ . In that case, Equation (24) can be written as (Bazant 1971, Xi 1994, Garrabrants and Kosson 2003):

$$\frac{\partial w}{\partial h} \frac{\partial h}{\partial t} - \text{div}(D_h \text{grad}(h)) = 0 \quad (26)$$

Again, the moisture diffusivity parameter is a nonlinear function that can be expressed as:

$$D_h = \lambda + \beta (1 - 2^{-10\gamma(h-1)}) \quad (\text{Xi 1994}) \quad (27)$$

$$D_h = D_{100\%} \left[ \alpha + \frac{1 - \alpha}{1 + \left( \frac{1-h}{1-h_c} \right)^n} \right] \quad (\text{Garrabrants and Kosson 2003}) \quad (28)$$

where:  $\lambda$ ,  $\beta$  and  $\gamma$  are parameters that need to be determined experimentally,  $D_{100\%}$  is the observed moisture diffusivity at 100% relative humidity,  $\alpha$  represents the ratio of  $D_{0\%}$  to  $D_{100\%}$ ,  $n$  is the spread in the drop of the S-shaped curve and  $h_c$  is a critical relative humidity corresponding to the center of the drop in the S-shaped curve.

### 2.3 Diffusion Potential

Many ionic transport models neglect the diffusion potential and the electrical coupling between ions. This is the case in groundwater modeling, where the ionic concentration levels are typically relatively low, at least compared to the pore solution of hydrated cement systems. Until recently, this was accepted as being applicable to ionic diffusion in concrete. However, some recent models are now considering coupling effects, assuming that the high concentration levels in the pores may cause strong concentration gradients, in which case the diffusion potential term in the mass conservation equation is no longer negligible. Some of these models will be reviewed when specific degradation mechanisms are addressed.

Two different approaches have been used to solve the diffusion potential variable. The first one relies on the null current density hypothesis  $\sum_i z_i j_i = 0$  to eliminate the potential from the transport equation. This approach was taken by Truc et al. (Truc 2000) and Masi et al. (Masi 1997). The diffusion potential can also be taken into account with the use of Poisson's equation that directly relates the potential to the concentration in solution. It is given here in its averaged form (Samson 2005):

$$\text{div}(w\tau \text{grad}(\Psi)) + w \frac{F}{\epsilon} \left( \sum_{i=1}^N z_i C_i \right) = 0 \quad (29)$$

where:  $\epsilon$  is the permittivity of the solution (usually assumed to be the same as water) and  $N$  is the total number of ionic species in aqueous phase. The coupling of Poisson's equation with the ionic transport relationship was used in references (Johannesson 2003, Samson 2007) to model ionic transport.

## 2.4 TEMPERATURE-FIELD MODELING

Different modeling approaches have been proposed to predict temperature distributions in porous materials. The most comprehensive approach consists of resolving the energy balance equation for each phase in the porous medium. This approach was used by Schrefler (Schrefler 2004) to model the temperature and humidity fields in concrete structures exposed to fire. The relationships are coupled through balance equations at the interfaces between each phase. However, these terms prove difficult to evaluate and are often neglected.

For most long-term durability analyses, the energy conservation equation can be simplified to the well-known heat conduction relationship:

$$\rho C_p \frac{\partial T}{\partial t} - \text{div}(k \text{grad} T) = 0 \quad (30)$$

where:  $\rho$  is the density of the material,  $C_p$  is the heat capacity, and  $k$  is the thermal conductivity. The thermal conductivity is a function of both the water content (saturation) and temperature (Kim 2003).

As emphasized in (Samson 2007), this relationship assumes that the heat of hydration effect are negligible after a few days, heat flow through convection caused by the fluid and gas movement in the material is negligible, and the heat capacity and conductivity parameter can be expressed as an average value of all the individual contribution of the various phases that compose the material. Equation (30) has been used by a few authors (Martin-Perez 2004, Saetta 1993) to evaluate the temperature field in concrete structures. However, temperature remains

a parameter that is generally neglected in many concrete durability analyses.

## 3.0 CHLORIDE INGRESS AND CORROSION

As mentioned in the previous, the ingress of chloride and its role in corrosion initiation is what prompted the development of the first models dedicated to long-term durability analyses of concrete structures. The following sections summarize the different mechanisms involved during chloride ingress and the modeling approaches described in the literature.

### 3.1 Chloride Interaction with Hydrated Cement Systems

It is generally accepted that the penetration of chloride ions in cement-based materials does not readily lead to the formation of detrimental solid phases that may cause expansion and cracking. On the contrary, the interaction between chloride in solution and the paste is often considered to have a beneficial influence on the durability of reinforced concrete since the paste binds penetrating ions, slowing the rate of ingress toward reinforcing steel.

Analysis of cement systems exposed to chloride shows that they react with the aluminate phases in the paste to form Friedel's salt:  $3\text{CaO} \cdot \text{Al}_2\text{O}_3 \cdot \text{CaCl}_2 \cdot 10\text{H}_2\text{O}$  (Barberon 2005, Brown 2000, Brown 2004, Mohammed 2004, Nielsen 2005, Suryavanshi 1998). This chloride bearing  $\text{AF}_m$  phase proved stable over a wide range of chloride concentrations (Birnin-Yauri 1998, Brown 2004): from a few mmol/L to greater than 3 mol/L.

Other phases have also been identified in synthetic cement systems, such as the chloro-sulfate  $\text{AF}_m$  phase called Kuzel's salt ( $3\text{CaO} \cdot \text{Al}_2\text{O}_3 \cdot \frac{1}{2}\text{CaCl}_2 \cdot \frac{1}{2}\text{CaSO}_4 \cdot 10\text{H}_2\text{O}$ ) (Glasser 1999). Although no data could be found for the stability of Kuzel's salt in presence of alkalis, the solubility data given in

reference (Glasser 1999) suggest that it only forms at low concentrations (< 10 mmol/L).

Various forms of calcium oxychlorides have been reported (Brown 2004) with the general composition of  $x\text{Ca}(\text{OH})_2 \cdot y\text{CaCl}_2 \cdot z\text{H}_2\text{O}$ . The compositions range from the simple 1:1:1 compound to more complex 4:1:10 or 3:1:12 assemblages. These chloride-bearing phases have mostly been observed in synthetic hydrated materials. But most importantly, oxychlorides observed in such laboratory conditions were only formed at very high chloride concentrations. For instance, the formation of the 3:1:12 phase requires approximately 4 mol/L of chloride while the 1:1:1 oxychloride is formed at a 9 mol/L chloride concentration (Brown 2004). In most practical cases, such as marine structures exposed to seawater or bridges and parking structures exposed to deicing salts, these concentration levels are not reached. It is thus doubtful that they form in structures unless chloride is concentrated by evaporation.

While many studies focused on the formation of Friedel's salt from hydrated  $\text{C}_3\text{A}$  systems, the role of Fe received very little attention. It is only recently that the formation of chloride-bearing minerals from hydrated  $\text{C}_4\text{AF}$  has raised interest. Suryavanshi et al. (Suryavanshi 1995) studied the binding of chloride in synthetic  $\text{C}_4\text{AF}$  hydrated with different levels of NaCl dissolved in the mix water. Chloride-bearing phases were identified using X-ray diffraction and differential scanning calorimetry. The results showed that a ferrite analogue to Friedel's salt was formed:  $\text{C}_3\text{F} \cdot \text{CaCl}_2 \cdot 10\text{H}_2\text{O}$ . This solid phase was also observed in (Csizmadia 2001) where pastes made of hydrated  $\text{C}_4\text{AF}$  and gypsum were exposed to a 10% NaCl solution over one-day wetting/drying cycles for durations between 28 and 56 days.

The previous paragraphs were concerned with the chemical interaction of chloride with hydrated cement paste. Chloride also physically interacts with cement-based materials due to interaction at the

pore solution/paste interface. In this case, new solid phases are not formed. Early binding experiments, such as the classical method devised by Luping and Nilsson (Luping 1993), give the overall amount of chloride that reacted with the material without making a distinction between physical and chemical interactions. But experiments with hydrated  $\text{C}_3\text{S}$  pastes (see for instance (Beaudoin 1990, Henocq 2006, Maltais 2004b) or synthetic C-S-H (Hong 1999) evidenced this phenomenon, since the absence of  $\text{C}_3\text{A}$  or  $\text{C}_4\text{AF}$  in these materials prevents the formation of Friedel's salt.

### 3.2 Binding Mechanisms

Many recent studies suggest that Friedel's salt formation is the result of chlorides reacting with hydrated phases such as monosulfates ( $\text{SO}_4\text{-AF}_m$ ). NMR results prompted Jones et al. (Jones 2003) to propose two different mechanisms for Friedel's salt formation: dissolution/precipitation and ionic exchange. The authors argue that both mechanisms are taking place simultaneously, and that the relative importance of each one depends on the chloride concentration in the pore solution.

Many studies suggest that the main mechanism is ionic exchange. Suryavanshi et al. (Suryavanshi 1996) were among the first to raise this hypothesis, on the basis of pore solution analyses. They concluded that the positive principal layer of hydroxy- $\text{AF}_m$   $\text{C}_4\text{AH}_{13}$  ( $[\text{Ca}_2\text{Al}(\text{OH})_6 \cdot n\text{H}_2\text{O}]^+$ ) releases an  $\text{OH}^-$  ion in the pore solution and replaces it with a free  $\text{Cl}^-$ . The relationship between hydroxy- $\text{AF}_m$  and Friedel's salt was further studied by Birnin-Yauri and Glasser (Birnin-Yauri 1998). Their results showed an almost complete solid solution between the two phases. Only a small solid miscibility gap was identified. Munshi et al. (Munshi 2005) based their chloride binding model on a complete exchange mechanism between  $\text{C}_4\text{AH}_{13}$  and chloride ions in the pore solution:



where: X represents ion exchange sites.

Ionic exchange was also proposed between sulfate AF<sub>m</sub> (monosulfate) and Friedel's salt (Hosokawa 2006). In this case, the proposed reaction releases sulfate in the pore solution upon chloride binding:



where: X represents ion exchange sites.

As mentioned in the previous section, the other mechanism responsible for chloride binding is physical interaction. In a recent paper, Henocq et al. (Henocq 2006) modeled the interaction of ions in the pore solution with the surface of C-S-H using double layer theory. The analysis showed that if a significant number of ions could be found in the diffuse layer, only a small fraction could be bound by specific

adsorption. The model predictions were found to correlate well with experimental data. Overall, the authors found that physical binding could account for only a small fraction of all ions bound by the cement paste.

Hosokawa devised a model that combines the monosulfate-based ionic exchange mechanism presented previously with a physical interaction model (Hosokawa 2006). As in the model developed by Henocq et al (Henocq 2006), physical interaction is attributable to surface complexation and the electrostatic interaction of ions with the surface of C-S-H is also considered. Results also confirm that chemical reactions contribute much more than physical interaction to the total amount of chlorides bound by hydrated cement systems (Figure 1).

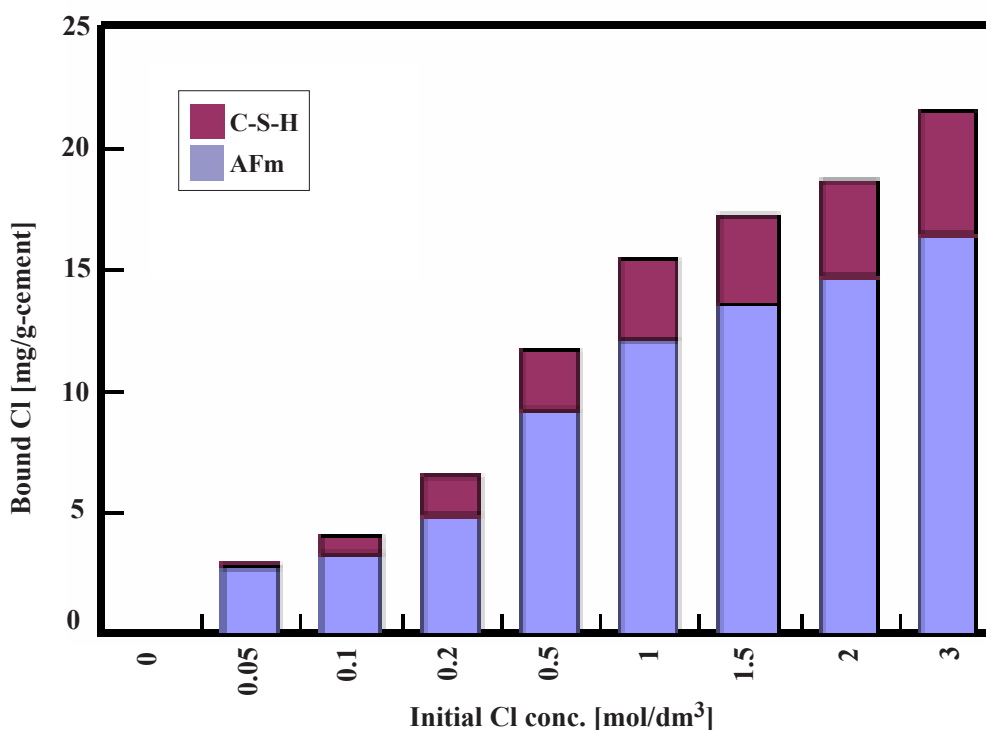


Figure 1. Contributions of the Chloride Chemical and Physical Binding In A Cement System (from (Hosokawa 2006))

### 3.3 Modeling Chloride Ingress

As previously emphasized, early models, developed about 30 years ago, were based on a single mass transport equation solely limited to chloride transport. Under the following assumptions: negligible electrical coupling and chemical activity effects, constant temperature, saturated material, no complexation reactions in the pore solution, and a linear relationship between bound and free chloride, Equation (6) can be simplified:

$$\frac{\partial C}{\partial t} - D_{app} \frac{\partial^2 C}{\partial x^2} = 0 \quad (33)$$

where:  $C$  is the chloride concentration in solution and  $D_{app}$  is the apparent diffusion coefficient.

This coefficient integrates both the diffusion characteristics of the material and the effect of chemistry on chloride penetration. It is important to note that according to the theory leading to Equation (6), the parameter  $C$  represents the chloride concentration in the pore solution. Under the assumption of constant  $D_{app}$  and boundary condition at  $x=0$ , there exist an analytical solution to Equation (33) in a semi-infinite domain ( $x \geq 0$ ):

$$C = C_o \operatorname{erfc} \left( \frac{x}{\sqrt{4D_{app}t}} \right) \quad (34)$$

where:  $C_o$  is the chloride level at  $x=0$ .

It should be emphasized that the validity of Equation (34) rests on a series of simplifying assumptions that are never met in reality.

Equation (34) has been used very loosely over the past decades. For instance, it has been noticed that measured chloride profiles have a shape similar to that of the profiles predicted by Equation (33). Experimental values have then been used to fit Equation (34) and determine  $C_o$  and  $D_{app}$  (see for instance (West 1985, Ghods 2005). In addition to the

questionable validity of Equation (33), this approach is also flawed because the variable  $C$  appearing in Eqs. (32) and (33) corresponds to the concentration of ions in the pore fluid, whereas Eq. (33) is often used to fit to experimental profiles of the total chloride content!

Although this method is based on very shaky scientific foundations, it is still being used to estimate the service life of partially saturated structures exposed to chloride-laden environments. In an attempt to refine the analysis, some authors have relied on the isotherm method to describe chemical reactions (Tang 1993). According to this approach, the amount of bound chlorides is linked to the chloride concentration in solution by an empirical function similar to the curve shown on Figure 1. This method does not allow a distinction between chemically and physically bound chlorides. By neglecting phenomena such as electrical coupling, chemical activity effects and Soret coupling, Equation (6) becomes:

$$\rho \frac{\partial C^b}{\partial C} \frac{\partial C}{\partial t} + \frac{\partial(wC)}{\partial t} - \operatorname{div}(wD \operatorname{grad}(C) - \mathbf{V}C) = 0 \quad (35)$$

where:  $C^b$  is the amount of bound chlorides and  $\rho$  is the density of the material. The term  $\partial C^b / \partial C$  corresponds to the slope of the binding isotherm curve.

This modeling approach has been used in (Hansen 1999, Martín-Pérez 2001, Nagesh 1998, Saetta 1993, Swaddiwudhipong 2000). Equation (35) can be coupled with the heat conduction Equation (30) to take into account the effect of temperature (Hansen 1999). It can also be combined with the moisture transport Equation (24) or (26) to evaluate the moisture flux  $\mathbf{V}$  and the water content (Nagesh 1998, Swaddiwudhipong 2000). Some authors also proposed models where Equation (35) is coupled to both moisture and temperature diffusion equations (Martín-Pérez 2001, Saetta 1993).

While the previous approaches can be considered to be improvements over Fick's second law of diffusion, they still neglect the interaction between the different ionic species present in solution. The current trend for ionic transport modeling focuses on multiionic approaches. For instance, models proposed by Masi et al. (Masi 1997) and Truc et al. (Truc 2000) consider that the transport of chlorides is coupled to that of other ionic species, using Equation (6). In these papers, the diffusion potential that couples the ionic species is solved using the null current condition:  $\sum_i z_i j_i = 0$ . The chloride interaction with the paste is based on an interaction isotherm that does not consider the presence of other ionic species.

In the model presented by Samson and Marchand (Samson 2007), chloride transport is based on the mass and energy conservation Equations (6), (24), (29) and (30). The model presented by the authors is based on a Sequential Non Iterative Approach where the transport equations and chemical reactions are solved separately. The chemical interaction of chlorides with the hydrated cement paste is based on an ionic exchange mechanism between monosulfates and Friedel's salt as in Equation (32). Typical simulation results are presented in Figure 2. The predicted total chloride content accounts for chloride ions present in the pore solution and those found in Friedel's salts.

### 3.4 Prediction of Corrosion Initiation

Reinforcing steel corrosion is mainly induced by the ingress of chlorides upon exposure to marine environment or deicing salts (Hope 1985). Due to the high pH of the concrete pore solution, the steel surface is naturally passivated. However, this protective layer can be destroyed in the presence of chlorides. Corrosion is initiated when the chloride concentration at the vicinity of the steel surface reaches a critical value, called the chloride threshold. This chloride threshold is usually expressed as a ratio between the concentration of chlorides and that of hydroxyl ions ( $[Cl^-]/[OH^-]$ ) or by the total amount

of chloride in the material (wt %) (Alonso 2000, Glass 1997, Hausmann 1967). A comprehensive review of threshold values is presented in (Alonso 2000). It shows a wide range of values depending on the characteristics of the mixture tested and on the test conditions. In most engineering analyses, the threshold value of 0.3% total chloride per cement weight (approximately 0.5g of total chloride per kg of concrete) specified by the Federal Highway Administration (USA) (FHWA 1998) is used.

The time needed to reach the critical chloride content for corrosion corresponds to the initiation period (Tuutti 1982). It is determined by a series of parameters such as the properties of the concrete cover, its thickness and the exposure conditions. Modeling the penetration of chloride ions within cement-based materials using an advanced modeling approach (see the previous section) can thus provide a proper way of predicting corrosion initiation if a reliable threshold can be estimated. Figure 3 illustrates a corrosion analysis based on the chloride ingress simulation showed in Figure 2. It presents the time evolution of the total chloride content at various locations within the concrete element, thus allowing the determination of the initiation time.

When the corrosion process is initiated, the formation of corrosion products can lead to stresses around the rebar that can damage the concrete cover. Different models develop to analyze this mechanical problem were reviewed in the mechanical damage report.

### 4.0 CARBONATION

The penetration of gaseous carbon dioxide within partially saturated concrete usually initiates a series of reactions with both ions dissolved in the pore solutions and the hydrated cement paste. The whole process can be summarized as a series of different steps: (1) gaseous carbon dioxide first penetrates the material, (2) gaseous carbon dioxide partitions in the pore solution mainly as  $HCO_3^-$  and  $CO_3^{2-}$ , and (3) the  $CO_3^{2-}$  species reacts with dissolved calcium

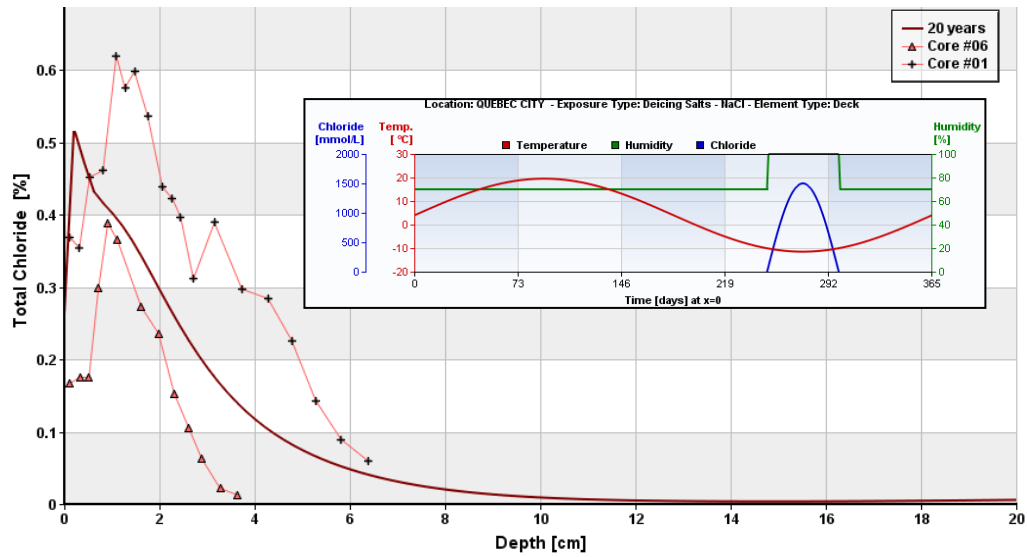


**Figure 2. Predicted Total Chloride Profile in a 20-year-old Parking Structure Using the Model Presented in (Samson 2007), Compared to Measurements Performed on Two Cores. (The inserted graph illustrates the time-dependent boundary conditions over one year.)**

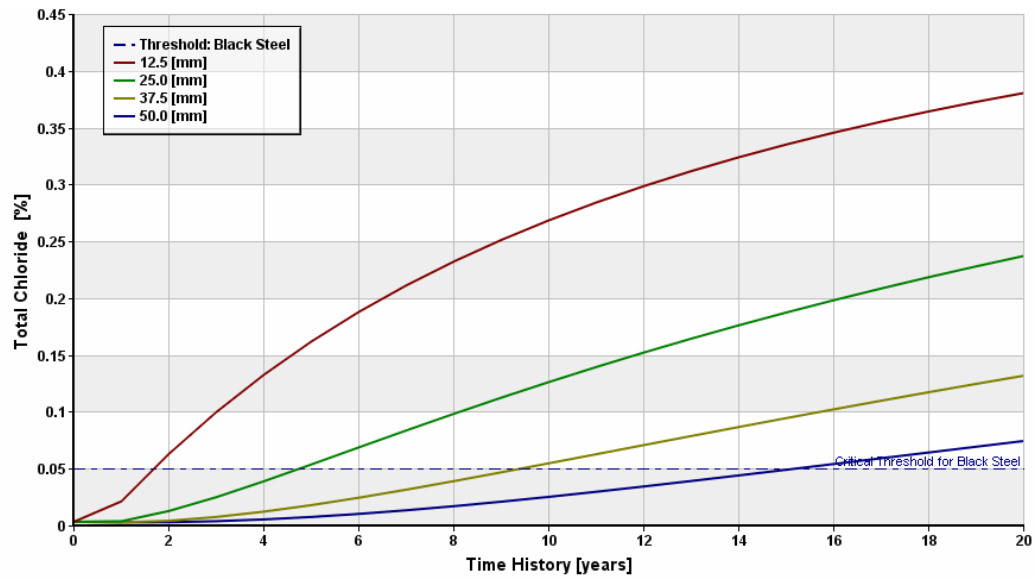


**Figure 3. Chloride Content at Different Rebar Positions (The calculations correspond to the case presented in Figure 2)**

to precipitate calcite,  $\text{CaCO}_3$ , as well as other  $\text{CO}_2$ -based solid phases. The consumption of calcium in solution leads to the dissolution of portlandite and an associated pH drop when portlandite is depleted.

The carbonation process itself does not have, *per se*, a negative effect on the paste physical properties. In some cases, it can even result in a reduction of the material porosity and favor formation of a protective layer at the surface of concrete. These physical effects increase retention of constituents (Gervais et al, 2004). However, the results of carbonation have been shown to increase leaching of some constituents, either through changes in constituent solubility resulting from neutralization of the material or through changes in speciation of constituents (Garrabrants et al 2004, Gervais et al 2004). Furthermore, the drop in pH associated with the process can potentially have a detrimental effect on reinforced concrete structures by destroying the passive layer around rebars. The next sections summarize different aspects of the carbonation process.

#### 4.1 Description of the Carbonation Process

Gaseous carbon dioxide partitions into the pore solution of cementitious materials as:



Under equilibrium conditions, the dissolution follows Henry's law, which is expressed in low (atmospheric) pressure environments as (Plummer 1982, Xu 2004):

$$\{\text{CO}_{2(aq)}\} = K_h P_{\text{CO}_2} \quad (37)$$

where:  $\{\text{CO}_{2(aq)}\}$  is the activity of the dissolved  $\text{CO}_{2(aq)}$ ,  $K_h$  is Henry's constant and  $P_{\text{CO}_2}$  is the partial pressure of  $\text{CO}_{2(g)}$  in the gas phase.

The temperature-dependent value of  $K_h$  can be expressed as (Plummer 1982):

$$\log K_h = 108.3865 + 0.01985076T - 6919.53/T - 40.45154 \log T + 669365.0 T^2 \quad (38)$$

where:  $T$  is the temperature.

Once in solution,  $\text{CO}_{2(aq)}$  dissociates into different ionic species according to the following reactions:



These reactions respectively obey the following equilibrium relationships:

$$K_1 = \{\text{H}^+\} \{\text{HCO}_3^-\} / \{\text{CO}_{2(aq)}\} \quad (41)$$

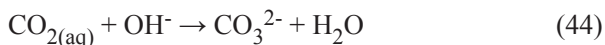
$$K_2 = \{\text{H}^+\} \{\text{CO}_3^{2-}\} / \{\text{HCO}_3^-\} \quad (42)$$

where: the brackets  $\{\dots\}$  indicate chemical activity. The time-dependent values for  $K_1$  and  $K_2$  are given in (Plummer 1982).

Using Equations (41) and (42) with the water dissociation relationship:

$$\{\text{H}^+\} \{\text{OH}^-\} = 10^{-14} \quad (43)$$

it is possible to estimate the fraction of each ionic species in solution as a function of the pH. This is illustrated by Figure 4. It shows that in cementitious materials, where pH values are usually high, the dominant species in solution is  $\text{CO}_3^{2-}$ . Barret et al. (Barret 1983) suggested that the reactions in Equations (39), (40) and (43) could be summarized by:



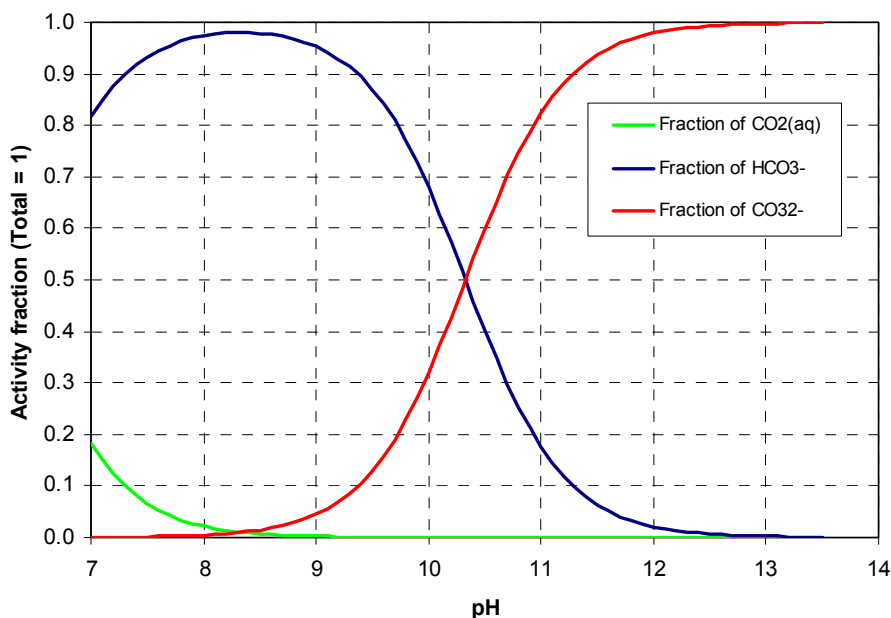


**Figure 4. Relative Distribution of  $\text{CO}_{2(\text{aq})}$ ,  $\text{HCO}_3^-$  and  $\text{CO}_3^{2-}$  as a Function of pH at 25°C**

This reaction illustrates that carbonation lowers pH by consuming hydroxide ions and producing water.

Once  $\text{CO}_3^{2-}$  is in the pore solution, it is free to react with other ionic species to precipitate carbonate phases. While aragonite and valerite polymorphs of  $\text{CaCO}_3$  have been reported, calcite ( $\text{CaCO}_3$ ) is generally identified as the main reaction product of carbonation (Papadakis 1991, Saetta 1993b) and precipitates according to the reaction:



where: the solubility constant has a value of  $\log(K)=-8.48$  at 25°C (Plummer 1982).

The presence of carbonates in solution can also lead to the formation of other solid phases. Barret et al. (Barret 1983) studied carbonation reactions by considering the formation of calcium hydrocarboaluminate  $3\text{CaO} \cdot \text{Al}_2\text{O}_3 \cdot \text{CaCO}_3 \cdot 11\text{H}_2\text{O}$ . The thermodynamic equilibrium of similar solid phases is described in two different papers (Damidot 1994, Damidot 1995).

According to Equations (44) and (45), the different mechanisms leading to the formation of calcite reduce the amount of calcium and hydroxide ions in the pore solution, which in turn triggers the dissolution of portlandite. The formation of calcite in replacement of portlandite reduces the porosity of the material since calcite has a higher molar volume ( $36.9 \text{ cm}^3/\text{mol}$  compared to  $33.1 \text{ cm}^3/\text{mol}$  for CH). Experimental evidence of calcium hydroxide reduction upon calcite formation was recently reported (Cultrone 2005, Rigo 2002). Neutralization of pore water alkalinity, precipitation of calcium carbonate and reduction in the calcium-silica ratio of the C-S-H are the end results of the carbonation process (Sanchez et al. 2002, Garrabrants et al. 2004, van Gerven et al. 2006, van Gerven et al. 2007). In tank leaching studies of solidified/stabilized (S/S) cementitious waste, carbonation from natural waters was shown to have the potential to alter both pH and concentration of species in the pore water (Sanchez et al. 2002, Garrabrants et al. 2004).

## 4.2 Carbonation Measurements

Carbonation depth is traditionally estimated using a phenolphthalein indicator. This is an indirect measure since the pink indicator actually shows where the pH drops below 9 by de-colorizing. Figure 5(a) presents mortar samples made at different water to cement ratios sprayed with phenolphthalein after 14 and 28 days of exposure to a 50% RH 5% CO<sub>2</sub> environment. Figure 5(b) shows that a plot of carbonation depths measured with phenolphthalein versus the square root of time yield a linear relationship. This is a common feature of the carbonation process (see for instance reference (Papadakis 1991)).

However, recent measurements showed that this technique only gives an approximate estimation of the depth of carbonation. Using a technique similar to the acid-dissolution approach for chloride profile measurements, Houst and Wittmann (Houst 2002) measured carbonate profiles in mortars exposed for 40 months to an outdoor environment. Results show that the carbonate profiles extend well beyond the depth indicated by phenolphthalein.

Similar measurements were reported by Baroghel-Bouny and Chaussadent (Baroghel-Bouny 2004). Calcite profiles were measured in paste samples

maintained in an accelerated carbonation room. Portlandite profiles were also determined.

Results show a drop of portlandite near the exposed surface, where the calcite content reaches its maximum value. According to these measurements, residual calcium hydroxide is still present near the solid/environment interface even though the material is carbonated.

## 4.3 Carbonation Models

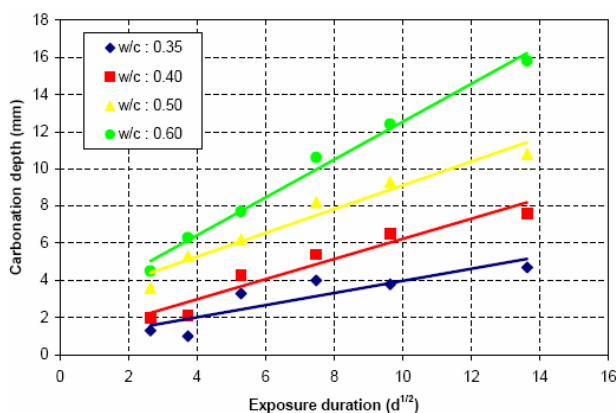
Numerous models dedicated to the prediction of the depth of carbonation can be found in the literature (Bary 2004, Cahyadi 1993, Saetta 1993b, Saetta 2004, Song 2006]. In all cases, the ingress of CO<sub>2(g)</sub> in the material is modeled using a diffusion-based equation:

$$\frac{\partial(\phi - w)[\text{CO}_{2(g)}]}{\partial t} - \text{div}((\phi - w)D_c \text{grad}[\text{CO}_{2(g)}]) - f_c = 0 \quad (46)$$

where:  $\phi$  is the porosity of the material,  $w$  is the volumetric water content,  $[\text{CO}_{2(g)}]$  is the gaseous carbon dioxide concentration,  $D_c$  is the gas diffusion coefficient and  $f_c$  is a sink term.



(a)



(b)

**Figure 5. Carbonation Depths (a) Measured with Phenolphthalein on Mortar Samples Exposed to a 50% RH 5% CO<sub>2</sub> Environment and (b) Plotted Against the Square Root of Time. (Data provided by SIMCO Technologies Inc.)**

In several proposed models (Bary 2004, Saetta 1993b, Saetta 2004, Song 2006), the parameter  $D_c$  is a function of the local water content in the material. In the approaches proposed by Saetta (Saetta 1993b, Saetta 2004) and Song (2006), the effect of temperature on gas transport is also considered. In Equation (46), the sink term  $f_c$  accounts for the transfer of carbon dioxide from the gaseous phase to the pore solution of the material (see Equation (36)).

Since gaseous carbon dioxide must enter the material to initiate the carbonation process, it is necessary to model the moisture transport process. The models cited previously are all based on Richards' Equation (24) or its relative humidity counterpart (26). In (Saetta 2004, Song 2006), a source/sink term is added to Equation (26) to model the hydration of the cement paste. This source/sink term in (Saetta 2004) also accounts for the formation of water involved in the carbonation process (see Equation (44)).

Based on Equations (46) and (24), it is possible to evaluate the amount of carbon dioxide in the pore solution  $\text{CO}_{2(\text{aq})}$ , and consequently the extent of the carbonation process. In most models, the reactions involved in the carbonation process are summarized as (Cahyadi 1993, Saetta 2004):



Simple rate equations are then used to calculate the formation of calcite or the loss of portlandite, such as (Saetta 1993b):

$$\frac{d[\text{CaCO}_{3(\text{s})}]}{dt} = f(w, T, [\text{Ca}(\text{OH})_{2(\text{s})}], [\text{CO}_{2(\text{aq})}]) \quad (48)$$

In (Bary 2004), the concentration of  $\text{Ca}^{2+}$  in solution is also taken into account, using an equation similar to (46). The source term represents the calcium that dissolves in solution when portlandite and C-S-H dissolve: it is assumed that  $\text{CO}_{2(\text{g})}$  dissolves in the pore solution as  $\text{CO}_3^{2-}$ . The amount of  $\text{CO}_3^{2-}$  in solution can be calculated from the source term in Equation (46), but the transport of this ionic species in solution

is neglected. Calcite is formed according to the equilibrium relationship:

$$[\text{Ca}^{2+}][\text{CO}_3^{2-}] = 10^{-8.35} \quad (49)$$

where: the square brackets [...] indicate concentrations. Calculations do not consider the presence of alkalis, since  $\text{Ca}^{2+}$  varies between 22 mmol/L (when portlandite is still present) to <1 mmol/L (upon complete decalcification of the C-S-H). In reference (Song 2006), the formation of calcite is modeled according to:

$$\frac{d[\text{CaCO}_{3(\text{s})}]}{dt} = k_r [\text{Ca}^{2+}][\text{CO}_3^{2-}] \quad (50)$$

where:  $k_r$  is a reaction rate.

The concentration of  $\text{CO}_3^{2-}$  follows Henry's law. The concentration of  $\text{Ca}^{2+}$  in the pore solution is calculated from a series of chemical equilibrium relationships. As in other references (e.g., Bary 2004), the movement of these species is not considered in the model, nor is the presence of alkalis.

This short review emphasizes the main shortcomings of most carbonation models. In most cases, the prediction of the pH drop is not part of the model since  $\text{OH}^-$  concentration is neglected. This is particularly detrimental when the risk of corrosion needs to be evaluated. Also, one of the main characteristic of cementitious materials, which is the highly alkaline pore solution, is neglected. From the chemical point of view, the presence of high  $\text{Na}^+$  and  $\text{K}^+$  concentrations are likely to significantly influence the carbonation process as they affect the chemical activity of the pore solution and consequently, chemical equilibrium with the hydrated paste.

## 5.0 DECALCIFICATION

The decalcification process is usually described by the dissolution of portlandite and C-S-H in hydrated cement systems exposed to pure water, even though dissolution can be observed in other environments

such as seawater. The leaching of ions (mainly calcium and hydroxide) from the pore solution to the external environment is primarily responsible for the dissolution of these hydrates. The decalcification phenomenon typically affects structures which have been in contact with pure or acidic waters for long time periods (e.g., dams, water pipes, radioactive waste disposal facilities). Over the past two decades, decalcification has been identified as a very relevant issue for nuclear waste storage (Berner 1992, Reardon 1992). The chemistry of attack has been described by Dow and Glasser (Dow 2003). It is shown how regimes of passivation and attack can be distinguished. The consequences of ionic leaching are an increase of the porosity and permeability, and a loss of mechanical strength. The leaching process from the stabilization and solidification of hazardous wastes standpoint has been reviewed in reference (Garrabrants 2005).

### 5.1 Description of the Process

The leaching of calcium is a coupled dissolution/diffusion process (Hinsenveld 1992, Sanchez 1996). Leaching by deionized water induces calcium and hydroxide concentration gradients that continuously decrease from the sound zone to the exposed surface of the material. This causes the diffusion of calcium and hydroxide ions from the pore solution to the aggressive solution, and thus lowers the amount of calcium concentration in the pore solution. Loss of calcium leads to the dissolution of portlandite and secondary precipitations of AFm, ettringite and calcite (Faucon 1997-98). The precipitation of these minerals takes place in the innermost part of the degraded zone while they are dissolved in the outermost part of the altered zone (Faucon 1997-98). But overall, the process mainly leads to the dissolution of calcium hydroxide and the decalcification of C-S-H (Adenot 1992, Faucon 1997, Haga 2005].

The altered material can be seen as a layered system composed of (Adenot 1992):

- An unaltered core delineated by total dissolution of portlandite,
- Different zones separated by dissolution or precipitation fronts ( $AF_m$ ,  $AF_t$ ...),
- Progressive decalcification of C-S-H.

The degraded zone induced by water exposure is characterized by a decalcification of C-S-H inducing a silicate polymerization. The Ca/Si ratio of the C-S-H gradually decreases between the sound and leached zones. Moreover, trivalent iron and aluminum from dissolved phases like  $AF_m$  and ettringite are incorporated into the C-S-H (Faucon 1996-97-98, Hidalgo 2007).

Cement hydrates in contact with water are dissolved depending on their solubility properties. According to their respective solubilities, hydrates dissolve successively in order to restore the chemical equilibrium between pore solution and crystallized hydrates. Properties of cement hydrate dissolution were characterized by Berner (Berner 1992) and Reardon (Reardon 1992) and new data, including hydrogarnet, siliceous hydrogarnet and strätlingite ( $C_2ASH_8$ ) are presented in (Matschei 2007). The solubilities of the main hydrated phases are classified in the following order:  $S_{Ca(OH)_2} > S_{AFm} > S_{\text{friedel's salt}} > S_{AFt}$  (Taylor 1997, Rémond 2002). The kinetics is influenced by the composition of the aggressive solution ( $CO_2$ , mineralized...) (Taylor 1997, Andac 1999, Moranville 2004, Maltais 2004) or by the saturation of the specimens (Maltais 2004).

As mentioned previously, calcium hydroxide is the main phase affected by the exposure to water. Calcium hydroxide depletion increases with the exposure period (Catinaud 2000, Saito 2000, Mainguy 2000, Yokozeki 2004, Haga 2005). Figure 6 shows the influence of the water-to-cement ratio on the dissolution kinetics. The amount of leached calcium increases with water-to-cement ratio (Saito 2000, Haga 2005). A higher value corresponds to a higher porosity (higher permeability and higher

pore volume) and a higher initial portlandite content (Moranville 2004, Haga 2005).

The increasing calcium concentration in solution is associated with a gradual penetration of the  $\text{Ca}(\text{OH})_2$  dissolution front Figure 6(b). The depth of penetration increases with water-to-cement ratio, which correlates with the results given in Figure 6(a) (Haga 2005).

Decalcification changes the bulk density and the pore structure of the hydrated cement paste. Haga et al. showed that the increase of pore volume is larger for a higher initial amount of  $\text{Ca}(\text{OH})_2$  (Haga 2005). This increase of pore volume is attributable to the dissolution of  $\text{Ca}(\text{OH})_2$  while the porosity created by C-S-H decalcification is negligible (Figure 7) (Carde 1996, Mainguy 2000, Haga 2005).

The use of supplementary cementing materials, combined with adequate curing, decreases the permeability of concrete and changes the kinetics of calcium leaching. Figure 8 shows the influence of blast-furnace slag and silica fume on calcium leaching (Saito 2000). The beneficial influence of both supplementary cementing materials is due to the reduction in the initial portlandite content (resulting

from the pozzolanic reaction) and to a significant reduction of the transport properties of the mixtures (Saito 2000, Moranville 2004).

The pore volume increase resulting from calcium leaching has a detrimental influence on the mechanical properties of cement-based materials. The relationship between pore volume and strength for sound and altered mortars was clearly shown by Saito and Deguchi Figure 9(a) (Saito 2000). Uniaxial compression tests on leached materials were performed by Carde et al. (Carde 1996). The total leaching of portlandite and the progressive decalcification of C-S-H led to a linear dependence of the strength on the ratio  $A_d/A_t$  between the degraded ( $A_d$ ) and the sound ( $A_t$ ) cross-sections Figure 9(b) (Carde 1996-97). The results shown on Figure 9 confirm the improvement of the leaching resistance associated with the use of supplementary cementing materials.

## 5.2 Experiments and Methods

Different test methods were developed to perform concrete decalcification experiments. Immersion tests in water (deionized or mineralized) are mainly used

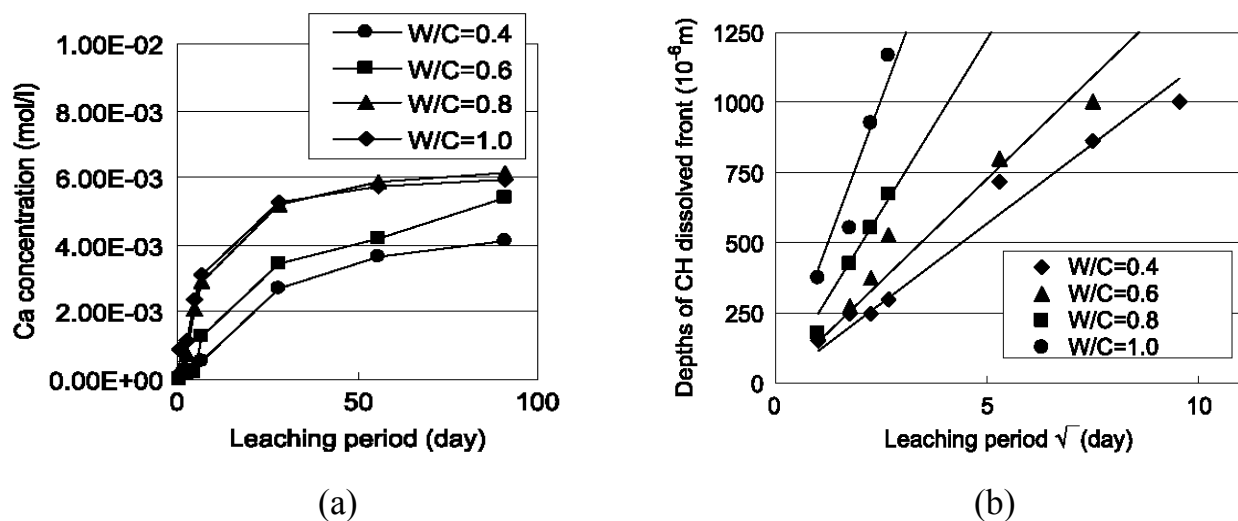


Figure 6. Change of  $\text{Ca}^{2+}$  Concentration as a Function of the Leaching Duration (a) and Depth of the  $\text{Ca}(\text{OH})_2$  Dissolved Front as a Function of the Square Root of the Leaching Period (b) (Haga 2005)

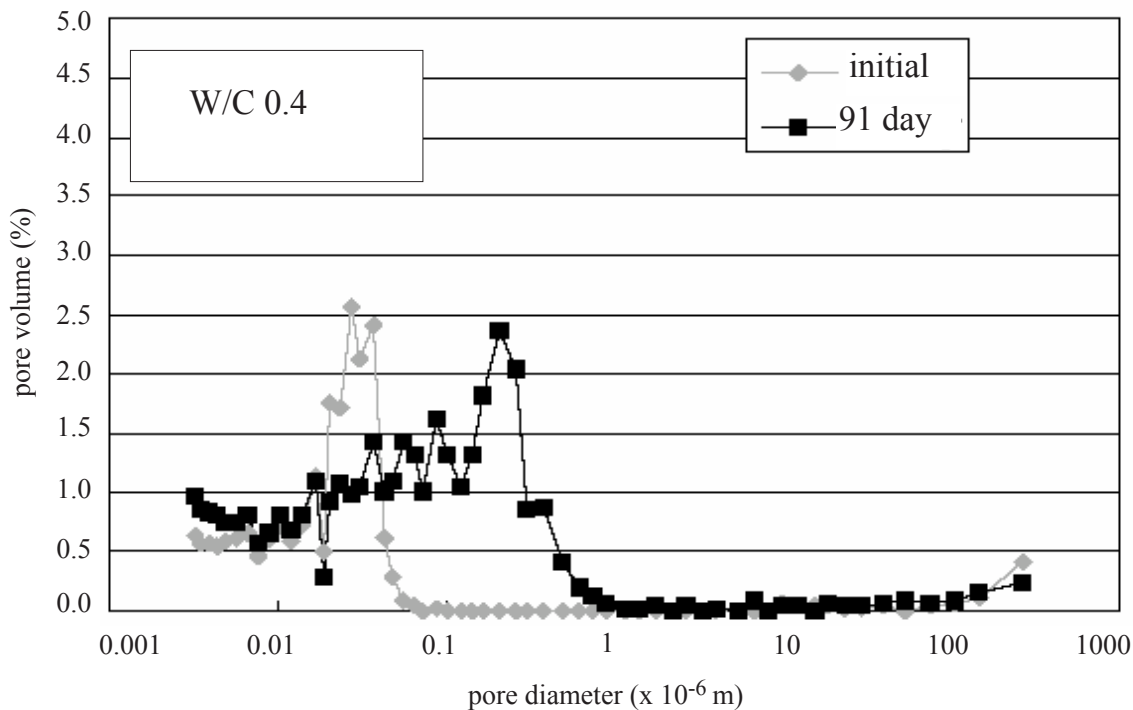


Figure 7. Pore Size Distribution on Sound and Leached Samples (Haga 2005)

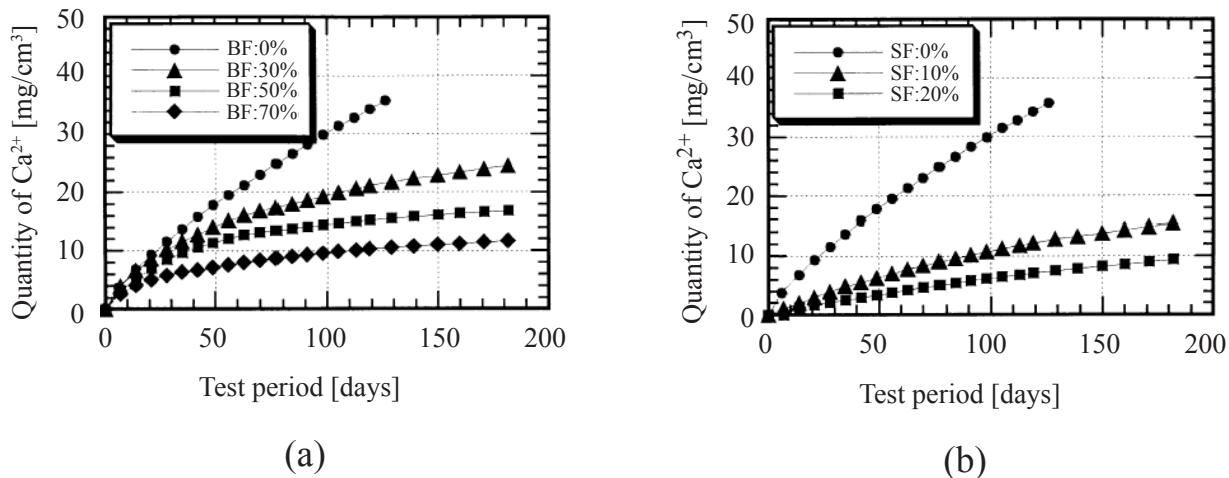
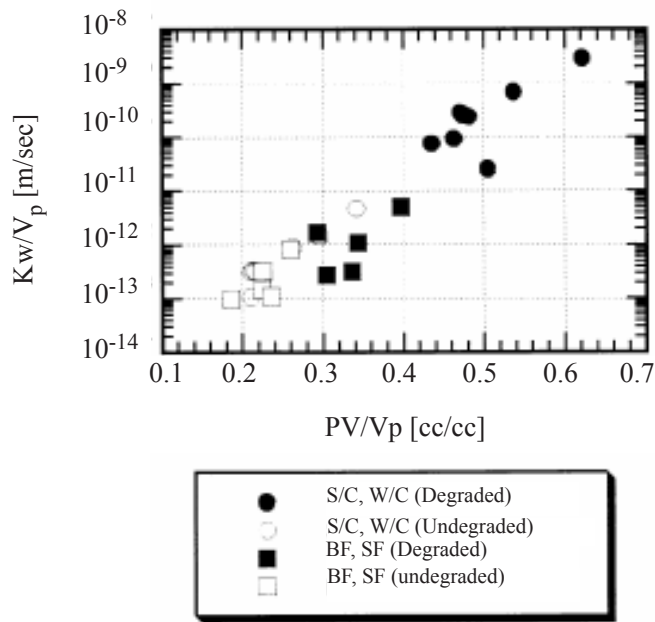
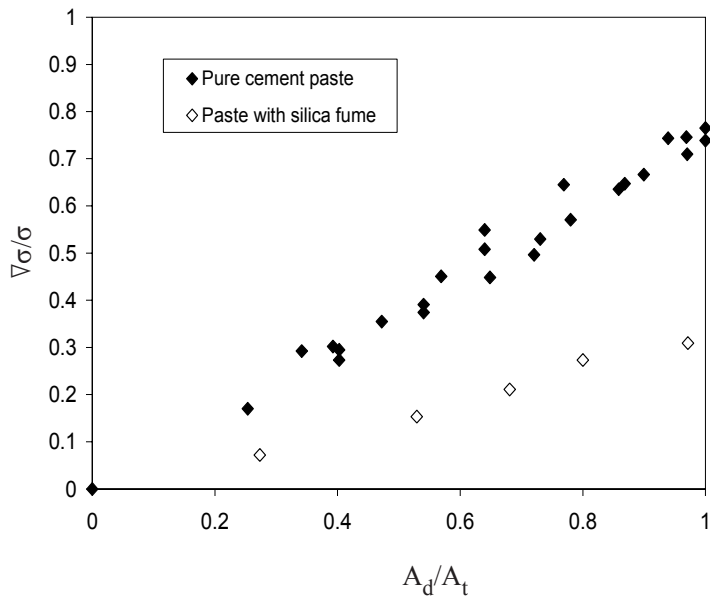


Figure 8. Cumulative Quantity of Dissolved Ca<sub>2+</sub> for SCM Mixtures (a) Blast-furnace Slag (BF) and (b) Silica Fume (SF) (Saito 2000)



(a)



(b)

**Figure 9. (a) Relationship Between Pore Volume ( $PV/V_p$ ) and Compressive Strength for Sound and Degraded Materials (Saito 2000) and (b) Variation of the Strength Loss in Relation to the Degradation Ratio  $A_d/A_t$  ( adapted from Carde 1996)**

for characterizing the leaching process (Faucon 1996, Mainguy 2000, Maltais 2004, Haga 2005). In some studies, tests were performed on ground material to measure the amount of leached calcium (Yokozeki 2004, Hidalgo 2007).

Since calcium leaching is a relatively slow process, a wide range of accelerated tests have been developed. The majority of these procedures are carried out with strongly acidified solutions (like ammonium nitrate) instead of deionized water (Carde 1996-97, Moranville 2004). In some cases, authors have also relied on organic acids to accelerate the leaching process (Bertron 2005). Finally, in some others, calcium leaching was accelerated by applying an electrical potential gradient across a specimen (Faucon 1998, Saito 2000)

### 5.3 Modeling the Decalcification Process

Calcium leaching in cement-based materials is a coupled chemical equilibrium/diffusion phenomenon. The kinetics and the mechanisms of this ionic transport process are described by Equation (6). Most models found in the literature are based on a simplified version of this equation (Mainguy 2000, Yokozeki 2004, Kuhl 2004, Haga 2005):

$$\phi(x,t) \frac{\partial C(x,t)}{\partial t} = D(x,t) \frac{\partial^2 C(x,t)}{\partial x^2} - \frac{\partial C_s(x,t)}{\partial t} \quad (51)$$

where:  $C(x,t)$  is the  $\text{Ca}^{2+}$  concentration in the liquid phase,  $C_s(x,t)$  is the content of Ca in solid phase,  $\phi(x,t)$  is the porosity and  $D(x,t)$  is the effective diffusion coefficient of  $\text{Ca}^{2+}$  ions.

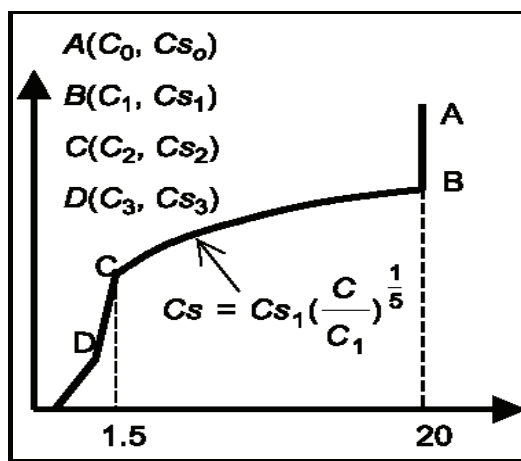
In Equation (51), the influence of phenomena such as chemical activity, convection and electrical coupling is neglected. The calcium content in solid  $C_s(x,t)$  is calculated from its relationship with calcium concentration in solution (Figure 10) (Mainguy 2000, Yokozeki 2004, Haga 2005). Another approach consists in determining the calcium content in the

solid by solving the chemical equilibrium between the minerals and the pore solution. The modeling of calcium leaching of hardened cement pastes in deionized water, by coupling Equation (6) and the dissolution/precipitation equilibrium of  $\text{Ca}(\text{OH})_2$  and C-S-H, was presented by Maltais et al. (Maltais 2004). The dissolution of portlandite and the decalcification of C-S-H were defined by their solubility constants  $K\text{Ca}(\text{OH})_2$  and  $K\text{CSH}$  respectively (Table 1).

The different leaching models take into account the evolution of the porosity of the material as solid phases dissolve. This increase of porosity as calcium is leached is given by (Maltais 2004, Yokozeki 2004, Kuhl 2004, Haga 2005):

$$\phi_{leaching} = \frac{M_{\text{Ca}(\text{OH})_2}}{d_{\text{Ca}(\text{OH})_2}} (C_{S,\text{Ca}(\text{OH})_2}^0 - C_{S,\text{Ca}(\text{OH})_2}) \quad (52)$$

This pore volume increase modifies the diffusion coefficient of calcium. Most empirical relationships linking the diffusion coefficient to porosity are similar to Equations (17) and (18). Others relationships are presented in Table 2.



Ca concentration in aqueous phase (C) ( $\times 10^{-3}$  mol/l)

**Figure 10. Relationship Between [Ca] in the Solution and the Solid Content from Daimon et al. (Haga 2005, Daimon 1977)**

**Table 1. Solubility Constants of Portlandite and C-S-H (Maltais 2004, Berner 1992)**

Name	Chemical Composition	Expression for Equilibrium ( $K_{sp}$ )	$-\log K_{sp}$
Portlandite	$\text{Ca(OH)}_2$	$\{\text{Ca}^{2+}\}\{\text{OH}^{-}\}^2$	5.2
C-S-H (Maltais 2004)	$0.65 \text{Ca(OH)}_2 + \text{CaH}_2\text{SiO}_4$	$\{\text{Ca}^{2+}\}\{\text{OH}^{-}\}^2$	6.2
C-S-H (Berner 1992, Henocq 2007)	$\text{CaH}_2\text{SiO}_4$ or $5\text{CaO} \cdot 5\text{SiO}_2 \cdot 10.5\text{H}_2\text{O}$	$\{\text{Ca}^{2+}\}\{\text{H}_2\text{SiO}_4^{2-}\}$ or $\{\text{Ca}^{2+}\}^5 \cdot \{\text{H}_3\text{SiO}_4^{-}\}^6 \cdot \{\text{OH}^{-}\}^4 / \{\text{H}_2\text{O}\}^{0.5}$	$f(C/S)^*$

\*  $-\log K_{sp}$  is a function of C/S ratio according to the empirical function  $f$ .

**Table 2. D = M(Ø) Relationships Found in Literature**

Cement Paste or Mortar	Relative Strength at 28 d	Maximum Temperature (% Reduction vs. Control)	Autogenous Shrinkage ( $\epsilon_{\min} - \epsilon_{\max}$ ) at 7 d and (% Reduction vs. Control)
$w/c = 0.35$ fine cement	100 %	66.9 °C (---)	-127 microstrains (---)
$w/c = 0.35$ coarse cement	74 %	47.4 °C (43 %)	-49 microstrains (61 %)
$w/c = 0.40$ fine cement	93 %	59.8 °C (16 %)	-100 microstrains (21 %)
$w/cm = 0.357$ fine cement/10 % fine limestone	93 %	58.8 °C (18 %)	-163 microstrains (-28 %)
$w/cm = 0.357$ fine cement/10 % coarse limestone	93 %	57.8 °C (20 %)	-88 microstrains (31 %)

Marchand et al. (Marchand 2001) proposed a direct relationship between a normalized diffusion coefficient  $D_N$  and the fraction of  $\text{Ca(OH)}_2$  (CH) leached:

$$D_N = 1 + \frac{1.1 \cdot CH^2}{0.28 + 0.79 \cdot CH} \quad (53)$$

where:  $D_N$  is defined as:

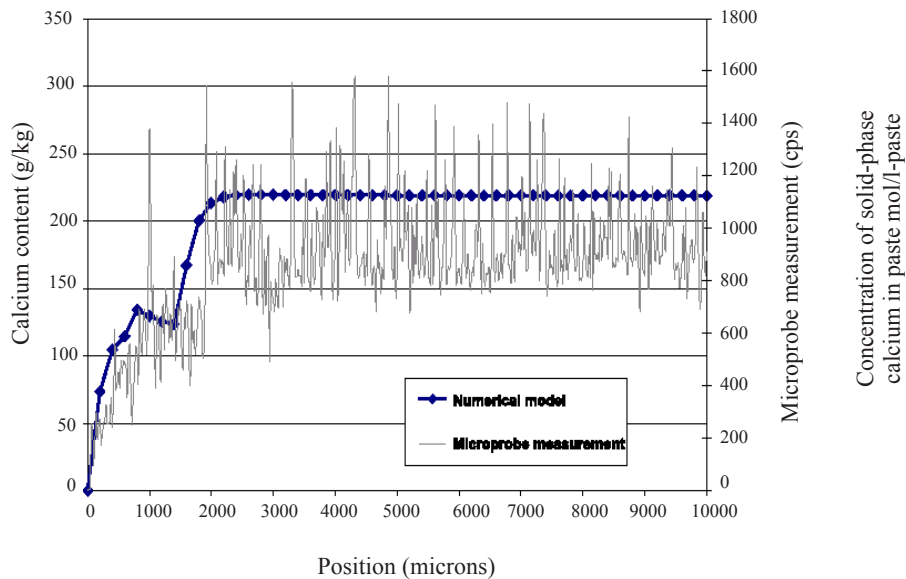
$$D_N = 1 + \frac{D(CH) - D(CH = 0)}{D(CH = 100) - D(CH = 0)}$$

Figure 11 shows simulations results compared to experimental data (Maltais 2004, Yokozeki 2004). The results in Figure 11(a) are obtained by solving Equation (6) coupled with chemical equilibrium while results in Figure 11(b) are determined by solving Equation (51) coupled with the calcium in solid phase relationship given by Figure 10.

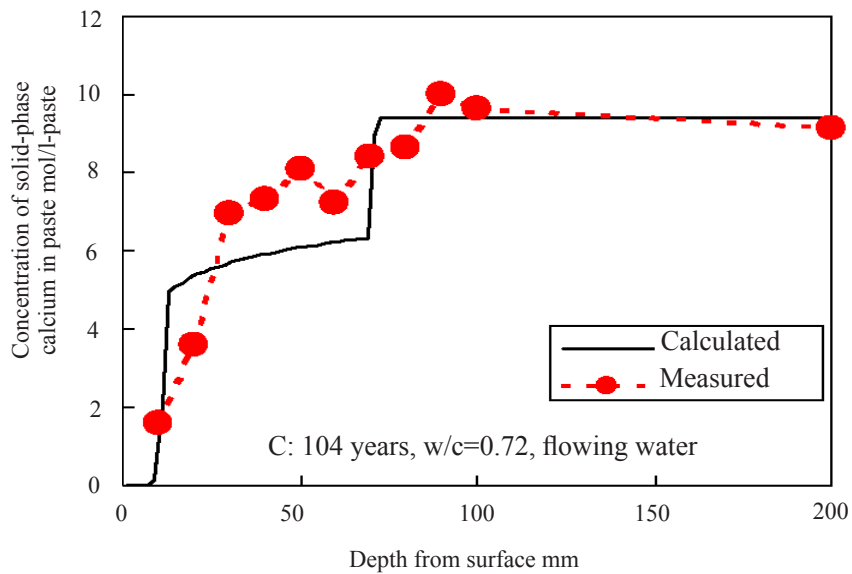
## 6.0 SULFATE ATTACK

Cement-based materials exposed to sulfate-bearing solutions such as some natural or polluted ground waters (external sulfate attack), or by the action of sulfates present in the original mix (internal sulfate attack) (Taylor 1997, Skalny 2002) can show signs of deterioration. Sulfate ions react with ionic species of the pore solution to precipitate gypsum ( $\text{CaSO}_4 \cdot 2\text{H}_2\text{O}$ ), ettringite ( $[\text{Ca}_3\text{Al(OH)}_6 \cdot 12\text{H}_2\text{O}]_2 \cdot (\text{SO}_4)_3 \cdot 2\text{H}_2\text{O}$ ) or thaumasite ( $\text{Ca}_3[\text{Si(OH)}_6 \cdot 12\text{H}_2\text{O}] (\text{CO}_3) \cdot \text{SO}_4$ ) (Taylor 1997) or mixtures of these phases. The precipitation of these solid phases can lead to strain within the material, inducing expansion, strength loss, spalling and severe degradation.

This section focuses on cementitious materials exposed to external sulfate sources only. The mechanical damages that can be induced upon



(a)



(b)

**Figure 11. Simulations of Calcium Leaching (a) on Cement Paste (Maltais 2004) and (b) on Mortar (Yokozeki 2004)**

external sulfate exposure are reviewed in the mechanical damage report.

### 6.1 Description of the Sulfate Attack Process

The ingress of sulfate ions into cementitious materials from  $\text{Na}_2\text{SO}_4$  or  $\text{K}_2\text{SO}_4$  sulfate-bearing solutions is generally coupled with calcium leaching since groundwaters are usually near the neutral state ( $\text{pH} \approx 7$ ). Depending on the conditions, this ingress may lead to the formation of gypsum in a layer close to the exposed surface in which calcium hydroxide is leached and/or reacted and the C-S-H phase is decalcified. Also, ettringite forms from monosulfate in a zone where calcium hydroxide is reduced (Skalny 2002, Maltais 2004, Brown 2000, Planel 2006, Dehwah 2007). In the presence of magnesium, the mechanism of sulfate ingress is different. In this case, the penetration of sulfate and magnesium ions is mainly characterized by the formation of brucite ( $\text{Mg}(\text{OH})_2$ ), an M-A-H phase resembling hydrotalcite, and a M-S-H gel. These replace C-S-H in addition to gypsum and ettringite formation. Particularly, the formation of M-S-H from C-S-H can result in more expansion and thus more degradation (Skalny 2002, Dehwah 2007, Higgins 2003).

The formation of gypsum and ettringite may lead to expansion and ultimately cracking. The formation of ettringite is often considered as the predominant cause of volume instability of hydrated cement systems in presence of sulfate solutions (Skalny 2002, Naik 2006). However, formation of gypsum was shown to cause expansion of C3S hydrated pastes and can probably contribute to the degradation of concrete in sulfate-laden environments (Tian 2000).

Many factors can influence the degradation of concrete by sulfate attack (Ouyang 1988). Water-to-cement ratio, for instance, has been found to have a significant effect on both the penetration of sulfate ions and the resulting expansion (Figure 12) (Ouyang 1988, Naik 2006, Skalny 2002, Lee 2005). This is

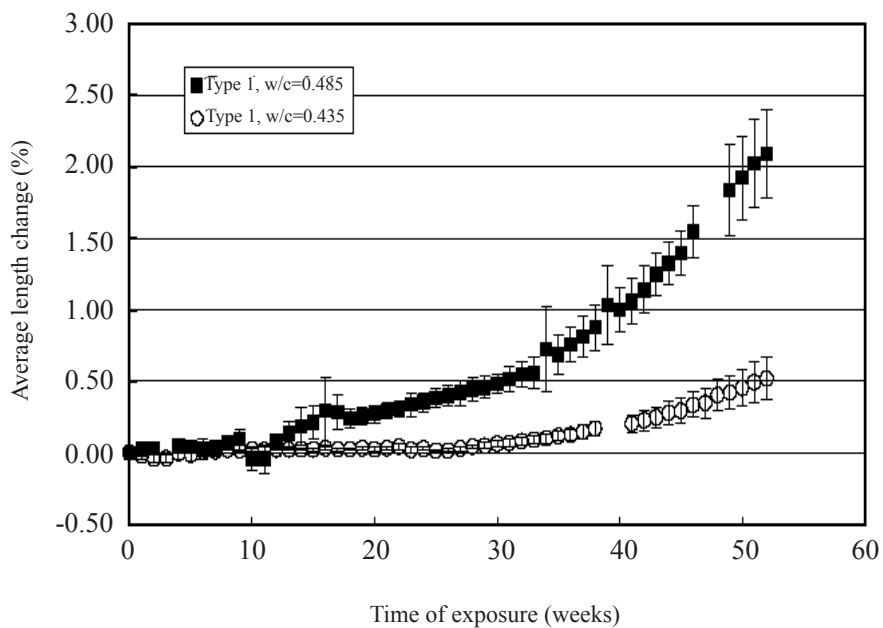
the reason why many standards limit the maximum water-to-cement ratio of concrete structures exposed to sulfates.

The mineralogy of cement, especially its C3A content and total aluminate content, is also known to influence the mechanisms of degradation. Expansion has been found to increase with the C3A content (Figure 13) (Ouyang 1988, Naik 2006, Skalny 2002, Odler 1999), which directly influences the amount of  $\text{AF}_m$  in the hydrated cement paste that reacts with sulfate ions to form ettringite.

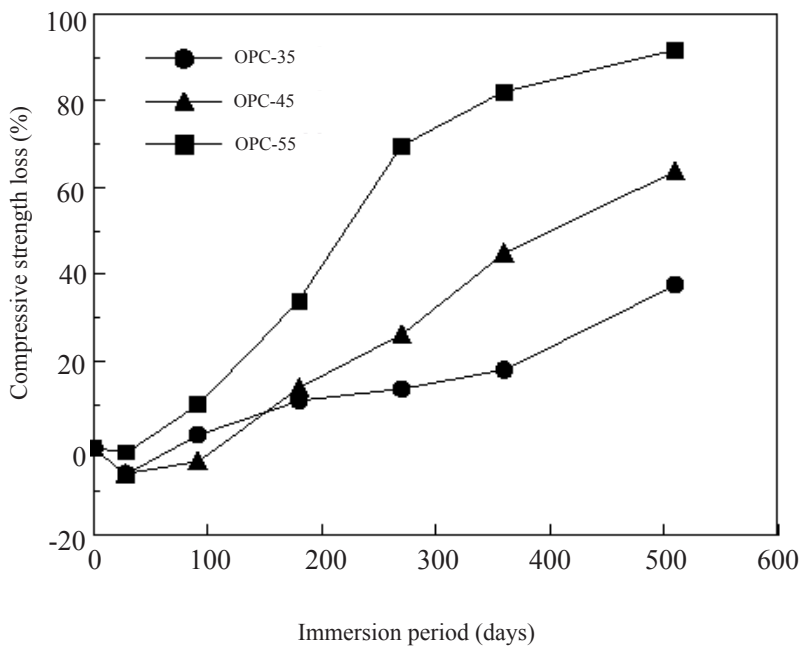
The presence of other ionic species also influences the product formed when concrete is exposed to sulfate. In the case of seawater for instance, the aqueous environment bears roughly 0.5M NaCl and 0.05M  $\text{MgSO}_4$ , with other species such as  $\text{K}_+$ ,  $\text{Ca}_{2+}$  and  $\text{HCO}_3^-$  present in small amount. In this environment, the formation of ettringite typically does not lead to expansion and cracking of the concrete and it is believed that the formation of this phase is non-expanding in the presence of excessive amounts of chloride ions (Skalny 2002).

As expected, concrete mixtures prepared with supplementary cementing materials show a better resistance to sulfate attack by reducing their permeability (Ouyang 1988, Lee 2005, Higgins 2003, Bakharev 2002). Metakaolin replacement (Al-Akhras 2006), silica fume (Lee 2005), slag (Higgins 2003, Bakharev 2002) and fly ash (Ouyang 1988) reduce the expansion of specimens undergoing sulfate attack. However, the ability of supplementary cementing materials to limit damage is much less significant in the presence of  $\text{MgSO}_4$  (Figure 14) (Higgins 2003).

The presence of sulfate ions can also lead to the formation of thaumasite. Such a phenomenon occurs when the following ions are present:  $\text{SO}_4^{2-}$ , C-S-H,  $\text{CO}_3^{2-}$ , in the presence of water (Taylor 1997, Bensted 1999, Crammond 2003). Numerous cases of field concrete degradation associated with thaumasite formation have been reported for

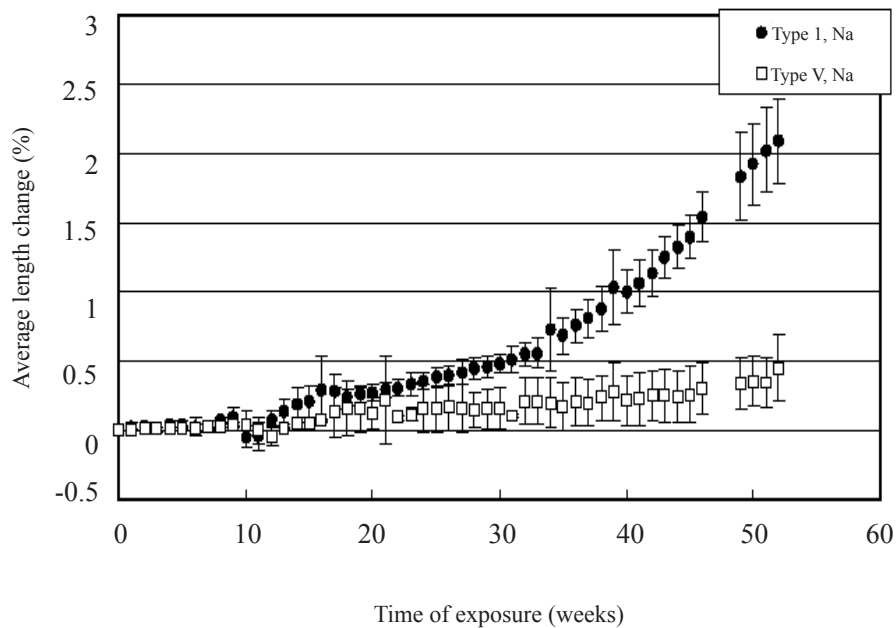


(a)

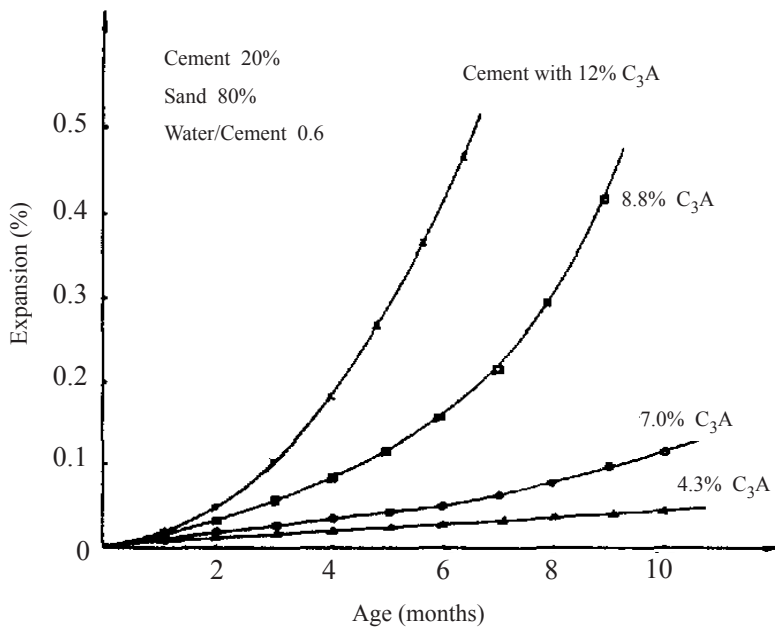


(b)

**Figure 12. Expansions of Mortars Under Sodium Sulfate Attack as A Function of W/C : (a) (Naik 2006) and (b) (Lee 2005)**

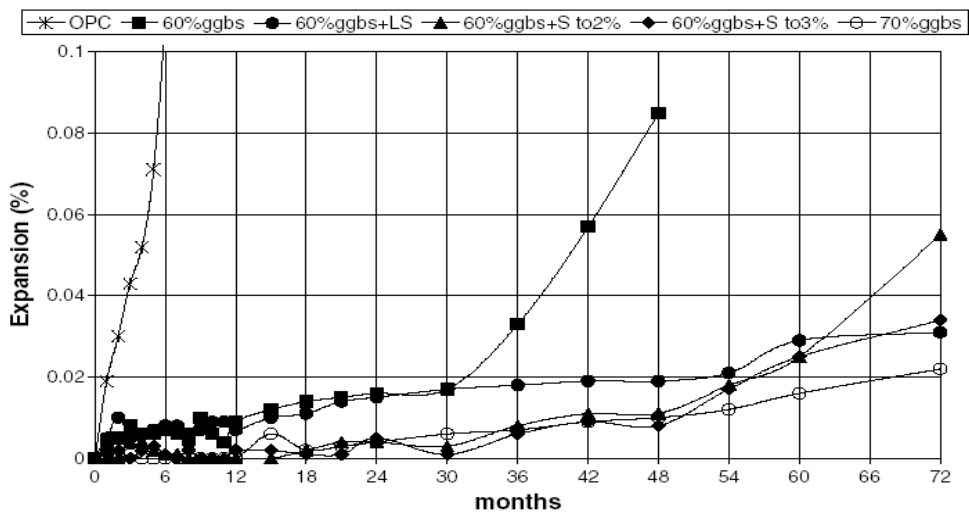


(a)

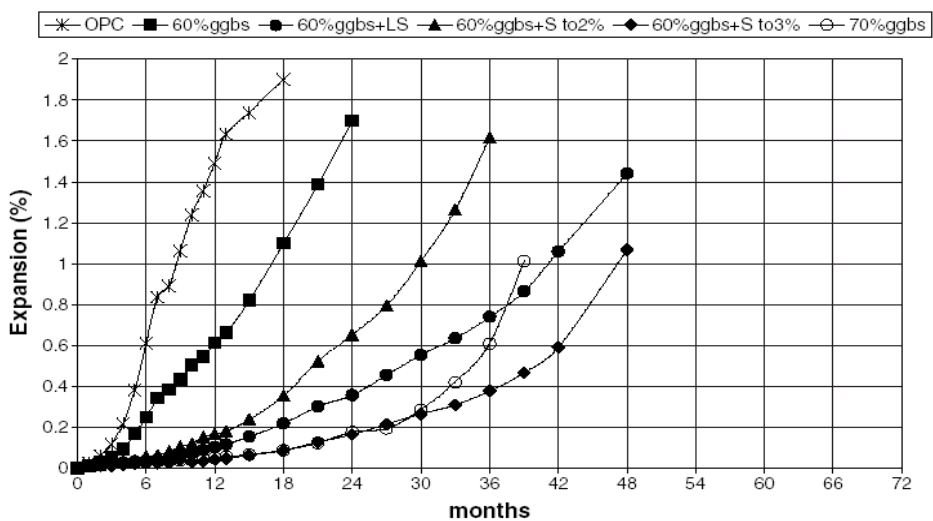


(b)

**Figure 13. Expansion of Mortars Under Sodium Sulfate Attack vs. C<sub>3</sub>A Content (a) %C<sub>3</sub>A type I > %C<sub>3</sub>A type V (Naik 2006) and (b) (Ouyang 1988)**



(a)



(b)

Figure 14. Expansions of Sandberg Prisms for Different Slag Contents (a) in  $\text{Na}_2\text{SO}_4$  Solution (1.5 %  $\text{SO}_3$ ) and (b) in  $\text{MgSO}_4$  Solution (1.5 %  $\text{SO}_3$ ) (Higgins 2003)

structures exposed to relatively low temperatures. This led some authors to believe that thaumasite was only stable at temperatures lower than  $\sim 10^{\circ}\text{C}$ . Higher temperatures, around  $20^{\circ}\text{C}$ , have been reported. Unexpected thaumasite was noted in warm climates such as California (Diamond 2003), Switzerland (Romer 2003) and Italy (Colleparidi 1999). Clearly, thaumasite forms readily at low temperature but cold temperatures are not an essential criterion (Collet 2004).

The influence of temperature on carbon dioxide solubility is a possible reason why thaumasite forms more readily at  $5^{\circ}\text{C}$  (Collet 2004). Moreover, Collet et al. assume that calcium bicarbonate, instead of calcium carbonate, would be the source of carbonate ions required for thaumasite formation (Collet 2004). C-S-H provides the source of silicate ions which react to form thaumasite. Thaumasite, which apparently has no capacity to act as a binder, gradually replaces C-S-H explaining why cementitious materials can be severely degraded by its formation (Taylor 1997, Santhanam 2001, Skalny 2002, Crammond 2003).

Two mechanisms have been proposed to describe the formation of thaumasite:

- Thaumasite forms from ettringite by substitution of  $\text{Al}^{3+}$  by  $\text{Si}^{4+}$  in the presence of  $\text{CO}_3^{2-}$  (Bensted 1999, Nobst 2003, Aguilera 2003, Pajares 2003),
- Thaumasite is the result of the direct interaction between C-S-H, sulfates and carbonates (Santhanam 2001, Aguilera 2003, Nobst 2003).

Thaumasite, when produced from ettringite and C-S-H mixtures, is not a pure mineral and contains other cations and anions in solid solution (Bensted 1999). More likely, thaumasite forms according to a through- solution process. As proposed by Crammond (Crammond 2003), ettringite can serve as a template for the initial nucleation of thaumasite. That would explain why some alumina is apparently beneficial

(Skalny 2002, Crammond 2003), even though thaumasite does not contain alumina. Overall, the ability of cements to allow thaumasite formation is said to be proportional to their  $\text{C}_3\text{A}$  or  $\text{Al}_2\text{O}_3$  contents (Nobst 2003).

Thaumasite formation is delayed in the case of concrete mixtures prepared with supplementary cementing materials. Influence varies with the type and the source of materials. Metakaolin and slag have been found to improve the behavior of limestone cements, showing that supplementary cementing materials offer an effective resistance if they react sufficiently quickly (Tsivilis 2003). However, mixtures prepared with fly ash, which is known to hydrate very slowly, remain vulnerable to thaumasite sulfate attack (Figure 15) (Mulenga 2003). The use of fly ash simply seems to retard sulfate attack (Tsivilis 2003). It is also important to note that since thaumasite does not contain alumina, “sulfate resistant” portland cement does not give an improvement of resistance against the formation of this deleterious phase (Skalny 2002, Mulenga 2003).

## **6.2 Experiments and Methods**

Various experimental approaches have been used to investigate the performance of hydrated cement systems exposed to sulfate solutions. Santhanam et al., have reviewed and criticized the different test methods proposed in the literature. Their analysis clearly emphasized the significant influence of experimental conditions (such as the control of pH, sulfate concentration and type of salts ( $\text{Na}_2\text{SO}_4$ ,  $\text{MgSO}_4$ ,  $\text{H}_2\text{SO}_4$ ...)) on the performance of test specimens (Santhanam 2001). Immersion tests in large volume or with renewed solutions are commonly used to maintain constant test conditions (Tian 2000, Maltais 2004, Bellmann 2006).

Microstructural alterations resulting from the exposure to sulfate-bearing solutions can be subsequently analyzed using different techniques such as microprobe analyses (Maltais 2004), SEM,

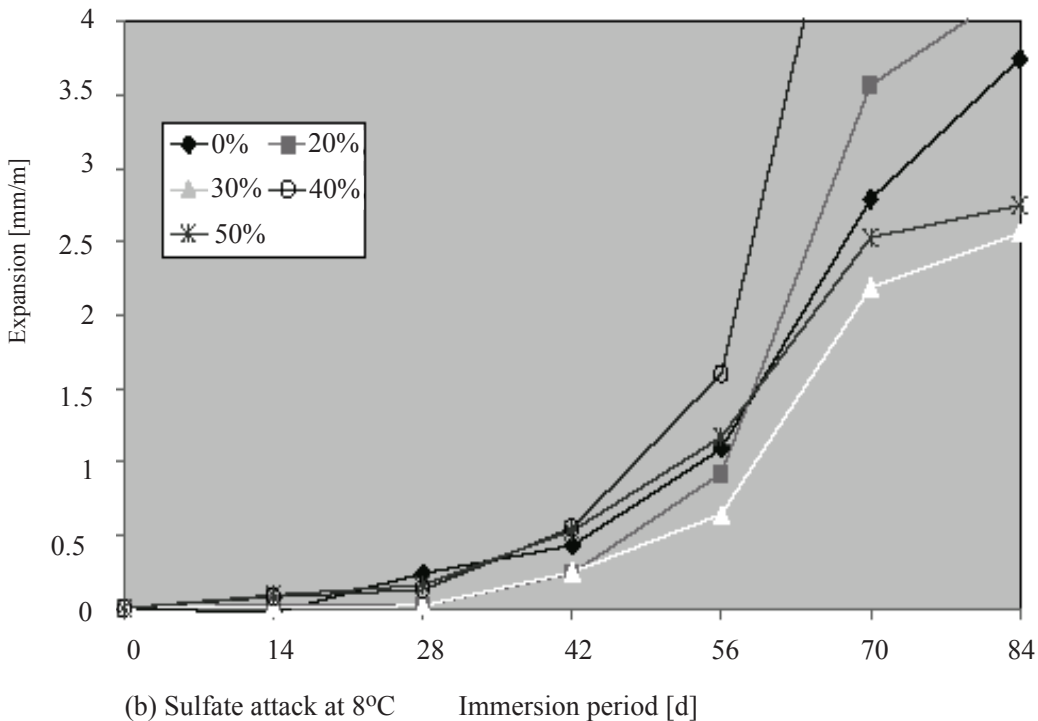
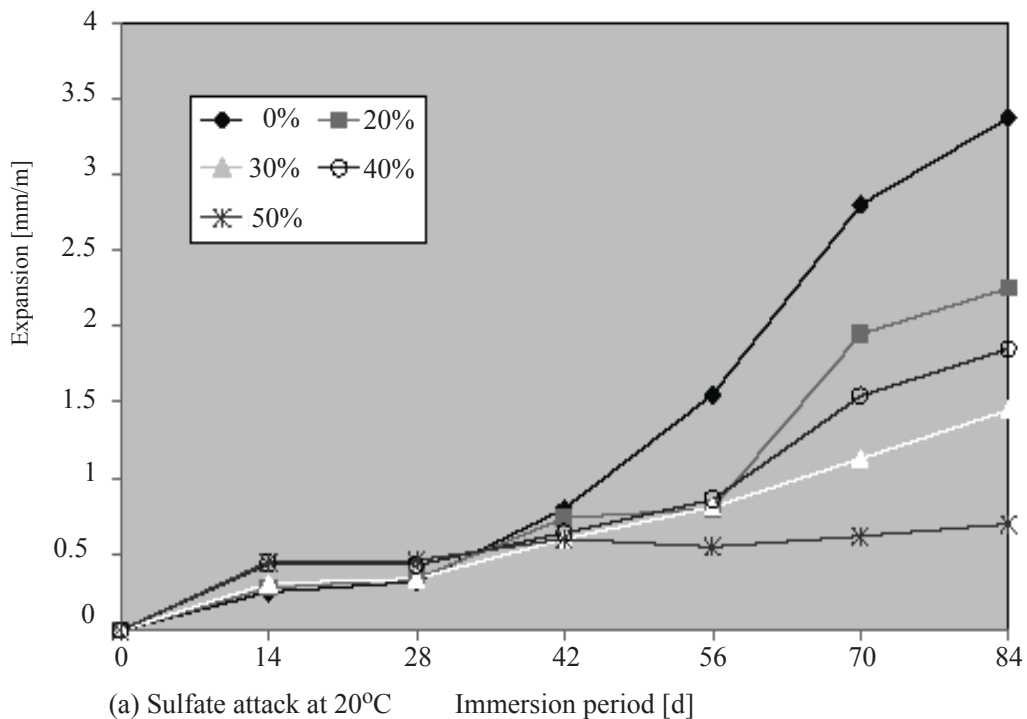


**Figure 15. Expansions of PLC Mortar Prisms Containing Fly Ash After Immersion in 4.4 % Sodium Sulfate Solution (Mulenga 2003)**

EDS and/or XRD for identifying crystallized phases (Brown 2000, Tian 2000). Naik et al., have also relied on X-ray microtomography and spatially resolved energy dispersive X-ray diffraction (EDXRD) to monitor the behavior of specimens exposed to sulfate solutions (Naik 2006). In some cases, damage induced by the exposure to sulfates can also be determined by compressive strength and/or volume change measurements (Ouyang 1988, Bakharev 2002, Higgins 2003, Naik 2006).

Most test methods used to investigate the resistance of cement systems to thaumasite formation are typically performed at around 5°C (Collet 2004, Zhou 2006, Heinz 2003, Hill 2003, Tsivilis 2003). However, some authors have also elected to investigate the influence of thaumasite by running tests at 20°C (Heinz 2003, Brown 2002, Tsivilis 2003, Mulenga 2003). Otherwise, thaumasite formation is mainly studied on field samples from different exposure conditions (Crammond 2003, Sibbick 2003, Diamond 2003, Romer 2003, Hobbs 2000-03, Loudon 2003). As thaumasite precipitation can occur in various environments, its solubility and its stability was respectively investigated from solid solutions by Macphee et al. (Macphee 2004) and in cement pastes by Juel et al. (Juel 2003).

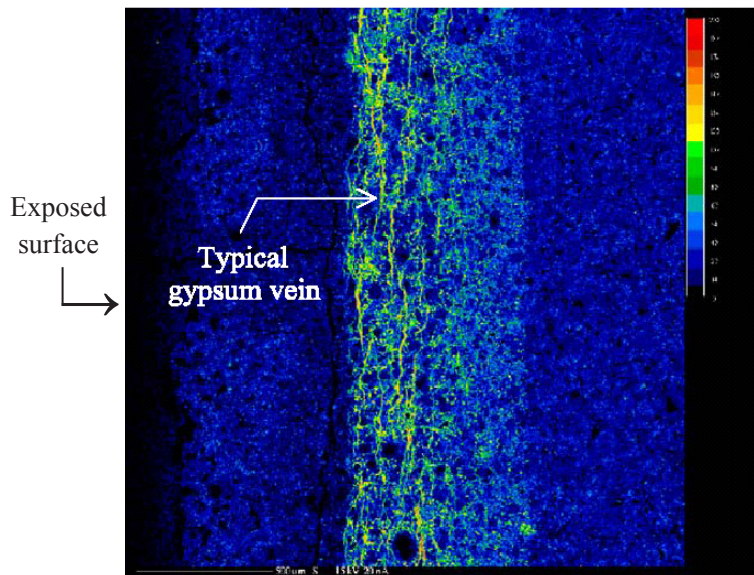
### **6.3 External Sulfate Attack Modeling**

Empirical, mechanistic and numerical models have been proposed in the literature for predicting the behavior of cement systems exposed to sulfate-laden environments. Empirical models estimate the sulfate resistance factor (Santhanam 2001), the expansion under sulfate attack (Kurtis 2000, Skalny 2002) or the location of the visible degradation zone (Skalny 2002). Mechanistic models typically attempt to take into account the mechanisms leading to the deterioration of the material. These models usually predict the rate of sulfate attack and the fractional or volumetric expansion (Skalny 2002). Ionic transport models simulate the chemical reactions occurring during sulfate attack and, in some cases, also estimate

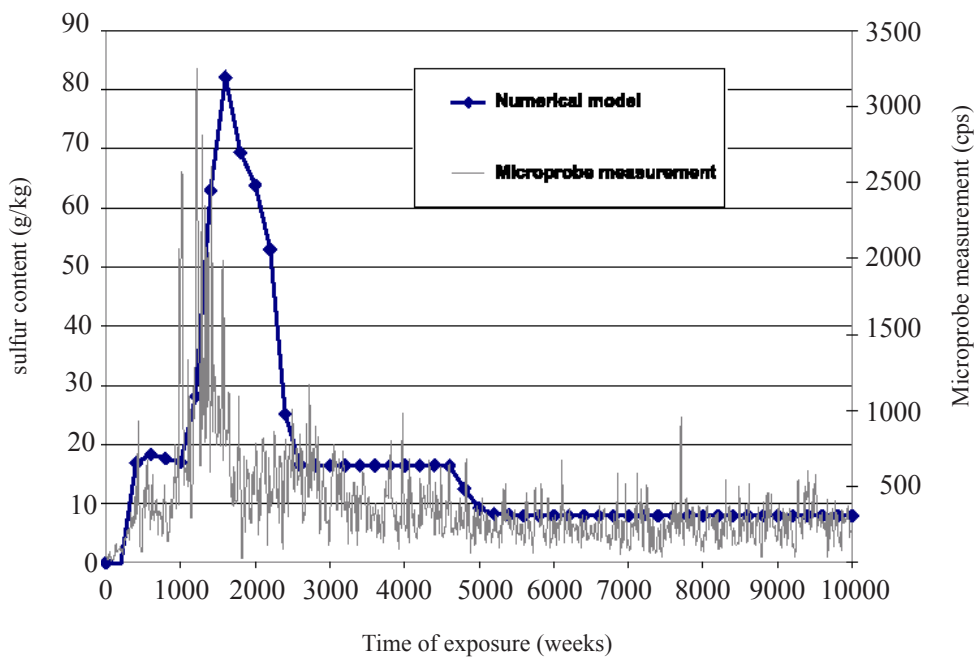
the damage caused by expansion (Skalny 2002, Marchand 2002, Maltais 2004).

The ability of empirical and mechanistic models to predict the behavior of concrete structures under sulfate attack remains somewhat limited. Ionic transport modeling offer a more detailed description of the process through dissolution-precipitation reactions coupled to transport of ions in cementitious matrix (see Equation 6). It is important to note that these models are inherently more complex than, for example, those used to describe chloride penetration. Since chloride ions interact only weakly with cement solids, diffusion profiles can in some cases be estimated from Fick's laws. Sulfate ions, however, react more strongly with cement substances and models need therefore to include mineralogical transformations. The complexity of the problem is increased by the fact that concrete structures in contact with a sulfate-bearing solution can not only be subjected to sulfate attack but are also usually affected by decalcification. The chemical reactions occurring under sulfate attack can be summarized by the solubility constants of ettringite, monosulfate and gypsum given in Table 3 when analyses are performed around 20°C (Maltais 2004).

Simulations of the chemical degradation by sodium sulfate solutions were presented by Maltais et al., Figure 16(b) (Maltais 2004) using a multiionic model that decouples transport and chemical reactions. As mentioned previously, the penetration of sulfate ions in cement-based materials can lead to the formation of a layer of gypsum at the vicinity of the exposed surface as shown in Figure 16(a). As can be seen in Figure 16(b), the multi-ionic model used in (ref. needed) could not only reproduce the sulfate distribution across the sample but was also capable of reliably predicting the distribution of all other solid phases within the material. These results provide a good example of the potential of numerical modeling to investigate the behavior of cement-based materials exposed to chemically-aggressive environments.



(a)



(b)

**Figure 16. Sulfur Content Mapping (a) and Sulfur Profiles (b) for 0.6 W/C Ratio CSA Type 10 Cement Pastes Exposed for 3 Months to a 50 mmol/l  $\text{Na}_2\text{SO}_4$  Solution (Maltais 2004)**

**Table 3. Solubility Constants of Solid Phases Involved During Sulfate Ingress in Hydrated Cement Systems (Maltis 2004))**

Name	Chemical Formula	Expression for Equilibrium ( $K_{sp}$ )	$-\log K_{sp}$
Ettringite	$3\text{CaO} \cdot \text{Al}_2\text{O}_3 \cdot 3\text{CaSO}_4 \cdot 32\text{H}_2\text{O}$	$\{\text{Ca}^{2+}\}^6 \{\text{OH}^-\}^4 \{\text{SO}_4^{2-}\}^3 \{\text{Al}(\text{OH})_4^-\}^2$	44.0
Monosulfate	$3\text{CaO} \cdot \text{Al}_2\text{O}_3 \cdot \text{CaSO}_4 \cdot 12\text{H}_2\text{O}$	$\{\text{Ca}^{2+}\}^4 \{\text{OH}^-\}^4 \{\text{SO}_4^{2-}\} \{\text{Al}(\text{OH})_4^-\}^2$	29.4
Gypsum	$\text{CaSO}_4 \cdot 2\text{H}_2\text{O}$	$\{\text{Ca}^{2+}\} \{\text{SO}_4^{2-}\}$	4.6

## 7.0 CONCLUSIONS

The present review emphasized that there are still many different approaches used to model ionic transport and chemical degradation in reactive cementitious materials. The situation is totally different from hydrogeology, where there is a general consensus around multiionic models considering multiple complexation and dissolution/precipitation reactions. While simplified approaches are still being used, it is acknowledged that they provide a simplified view of the complex mechanisms involved.

For cementitious materials, the mechanistic models have not received the same kind of support. Consequently, they are only marginally recognized as potent tools to make long-term service-life predictions of concrete structures. Despite this lack of support, multiionic models for cementitious materials have been developed to predict the chemical degradation for sulfate or decalcification exposure cases.

The situation is worse for chloride ingress modeling. In that case, simplified models are not only widely used but based on an incorrect interpretation of

the mass conservation equation. The most glaring problem with the simplified approach occurs with the use of the analytical solution to Fick's second law for chloride ingress analyses. In most cases, the total chloride content in the material is directly substituted to the chloride concentration in the pore solution, which violates the mass conservation equation at the origin of the model. Most importantly, this leads to the determination of a parameter called the apparent diffusion coefficient which does not only characterize the material but also incorporate the local exposure conditions. However, a limited number of studies based on more reliable multiionic models have been published recently.

Finally, carbonation models reviewed in this report were all based on simplified approaches. The complex interactions between gaseous carbon dioxide, the pore solution and the mineral phases such as calcite and portlandite have not so far been implemented in a mechanistic approach. A mechanistic modeling framework considering gas and ionic transport in cementitious material coupled with complex chemical reaction capabilities would be a step forward compared to existing models.

## 8.0 REFERENCES

Adenot, F & Buil, M 1992, 'Modelling of the corrosion of the cement paste by deionized water', *Cement and Concrete Research*, vol. 22, pp. 489-496.

Aguilera, J Martinez-Ramirez, S Pajarez-Colomo, I & Blanco-Varela, MT 2003, 'Formation of thaumasite in carbonated mortars', *Cement & Concrete Composites*, vol. 25, pp. 991-996.

Al-Akhras, NM 2006, 'Durability of metakaolin concrete to sulfate attack', *Cement and Concrete Research*, vol. 36, pp. 1727-1734.

Alonso, C Andrade, C Castellote, C & Castro, P 2000, 'Chloride threshold values to depassivate reinforcing bars embedded in a standardized OPC mortar', *Cement and Concrete Research*, vol. 30, pp.1047-1055.

Andac, M & Glasser, FP 1999, 'Long-term leaching mechanisms of portland cement-stabilized municipal solid waste fly ash in carbonated water', *Cement and Concrete Research*, vol. 29, pp. 179-186.

Bakharev, T Sanjayan, JG & Cheng, YB 2002, 'Sulfate attack on alkali-activated slag concrete', *Cement and Concrete Research*, vol. 32, pp. 211-216.

Barberon, F Baroghel-Bouny, V Zanni, H Bresson, B d'Espinose de la Caillerie, JB Malosse, L & Zehong, G 2005, 'Interactions between chloride and cement-paste materials', *Magnetic resonance Imaging*, vol. 23, pp. 267-272.

Baroghel-Bouny, V & Chaussadent, T 2004, 'Transferts dans les bétons et durabilité des ouvrages', *Bull. Lab. Ponts et Chaussées*, vol. 248, pp. 93-111 (in French).

Barret, P Bertrandie, D & Beau, D 1983, 'Calcium hydrocarboaluminate, carbonate alumina gel and hydrated aluminates solubility diagram calculated in equilibrium with CO<sub>2g</sub> and with Na<sup>+</sup><sub>aq</sub> ions', *Cement and Concrete Research*, vol. 13, pp. 789-800.

Bary, B & Sellier, A 2004, 'Coupled moisture - carbon dioxide - calcium transfer model for carbonation of concrete', *Cement and Concrete Research*, vol. 34, pp. 1859-1872.

Bazant, ZP Najjar, LJ 1971, 'Drying of concrete as a nonlinear diffusion problem', *Cement and Concrete Research*, vol. 1, pp. 461-473.

Bear, J Bachmat, Y 1991, *Introduction to Modeling of Transport Phenomena in Porous Media*, Kluwer Academic Publishers, The Netherlands.

Beaudoin, JJ Ramachandran, VS & Feldman, RF 1990, 'Interaction of chloride and C S H', *Cement and Concrete Research*, vol. 20, pp. 875-833.

Bellmann, F Möser, B & Stark, J 2006, 'Influence of sulfate solution concentration on the formation of gypsum in sulfate resistance test specimen', *Cement and Concrete Research*, vol. 36, pp. 358-363.

Bensted, J 1999, 'Thaumasite – background and nature in deterioration of cements, mortars and concretes', *Cement & Concrete Composites*, vol. 21, pp. 117-121.

Berner, UR 1992, 'Evolution of pore water chemistry during degradation of cement in a radioactive waste repository environment', *Waste Management*, vol. 12, pp. 201-219.

Bertron, A Duchesne, J & Escadeillas, G 2005, 'Accelerated tests of hardened cement pastes alteration by organic acids: analysis of the pH effect', *Cement and Concrete Research*, vol. 35, pp. 155-166.

- Birnin-Yauri, UA & Glasser, FP 1998, 'Friedel's salt,  $\text{Ca}_2\text{Al}(\text{OH})_6(\text{Cl},\text{OH})\cdot\text{H}_2\text{O}$ : its solid solutions and their role in chloride binding', *Cement and Concrete Research*, vol. 28, pp. 1713-1723.
- Bockris, JO'M & Reddy, AKN 1970, *Modern Electrochemistry – An Introduction to an Interdisciplinary Area*, Plenum Press, USA.
- Brown, PW & Badger, S 2000, 'The distribution of bound sulfates and chlorides in concrete subjected to mixed  $\text{NaCl}$ ,  $\text{MgSO}_4$ ,  $\text{Na}_2\text{SO}_4$  attack', *Cement and Concrete Research*, vol. 30, pp. 1535-1542.
- Brown, P & Hooton, RD 2002, 'Ettringite and thaumasite formation in laboratory concretes prepared using sulfate-resisting cements', *Cement & Concrete Composite*, vol. 24, pp. 361-370.
- Brown, P & Bothe, J 2004, 'The system  $\text{CaO}-\text{Al}_2\text{O}_3-\text{CaCl}_2-\text{H}_2\text{O}$  at  $23\pm 2^\circ\text{C}$  and the mechanisms of chloride binding in concrete', *Cement and Concrete Research*, vol. 34, pp. 1549-1553.
- Cahyadi, JH & Uomoto, T 1993, 'Influence of environmental relative humidity on carbonation on concrete (mathematical modeling)', *Durability of Building Materials and Components*, vol. 6, edited by S. Nagataki, pp. 1142-1151.
- Carde, C François, R & Torrenti, J-M 1996, 'Leaching of both calcium hydroxide and C-S-H from cement paste: modeling the mechanical behavior', *Cement and Concrete Research*, vol. 26, no. 8, pp. 1257-1268.
- Carde, C & François, R 1997, 'Aging damage model of concrete behavior during the leaching process', *Materials and Structures*, vol. 30, pp. 465-472.
- Catinaud, S Beaudoin, JJ & Marchand, J 2000, 'Influence of limestone addition on calcium leaching mechanisms in cement-based materials', *Cement and Concrete Research*, vol. 30, pp. 1961-1968.
- Colleparidi, M 1999, 'Thaumasite formation and deterioration in historic buildings', *Cement & Concrete Composites*, vol. 21, pp. 147-154.
- Collet, G Crammond, NJ Swamy, RN & Sharp, JH 2004, 'The role of carbon dioxide in the formation of thaumasite', *Cement and Concrete Research*, vol. 34, pp. 1599-1612.
- Crammond, N.J. 2003, 'The thaumasite form of sulfate attack in the UK', *Cement and Concrete Composites*, vol. 25, pp.809-818.
- Csizmadia, J Balázs, G & Tamás, FD 2001, 'Chloride ion binding capacity of aluminoferrites', *Cement and Concrete Research*, vol. 31, pp. 577-588.
- Cultrone, G Sebastian, E & Huertas, MO 2005, 'Forced and natural carbonation of lime-based mortars with and without additives: Mineralogical and textural changes', *Cement and Concrete Research*, vol. 35, pp. 2278-2289.
- Daimon, M Abo-El-Enein, SA Hosaka, G Goto, S & Kondo, R 1977, 'Pore structure of calcium silicate hydrate in hydrated tricalcium silicate', *J. Am. Ceram. Soc.*, vol. 60, no. 3-4, pp. 110-114.
- Damidot, D Stronach, S Kindness, A Atkins, M & Glasser FP 1994, 'Thermodynamic investigation of the  $\text{CaO}-\text{Al}_2\text{O}_3-\text{CaCO}_3-\text{H}_2\text{O}$  closed system at  $25^\circ\text{C}$  and the influence of  $\text{Na}_2\text{O}$ ', *Cement and Concrete Research*, vol. 24, pp. 563-572.
- Damidot, D & Glasser, FP 1995, 'Thermodynamic investigation of the  $\text{CaO}-\text{Al}_2\text{O}_3-\text{CaSO}_4-\text{CaCO}_3-\text{H}_2\text{O}$  closed system at  $25^\circ\text{C}$  and the influence of  $\text{Na}_2\text{O}$ ', *Advance in Cement Research*, vol. 7, pp. 129-134.
- Degiovanni, A & Moyne, C 1987, 'Conductivité thermique de matériaux poreux humides: évaluation théorique et possibilité de mesure', *Int. J. Heat Mass Transfer*, vol. 30, pp. 2225-2245 (in French).

- Dehwah, HAF 2007, 'Effect of sulfate concentration and associated cation type on concrete deterioration and morphological changes in cement hydrates', *Construction and Building Materials*, vol. 21, pp. 29-39.
- Diamond, S 2003, 'Thaumasite in Orange County, Southern California: an inquiry into the effect of low temperature', *Cement & Concrete Composites*, vol. 25, pp. 1161-1164.
- Dow, C & Glasser, FP 2003, 'Calcium carbonate efflorescence on Portland cement and building materials', *Cement and Concrete Research*, vol. 33, pp. 147-154.
- Emmanuel, S & Berkowitz, B 2005, 'Mixing-induced precipitation and porosity evolution in porous media', *Adv. Water Res.*, vol. 28, pp. 337-344.
- Faucon, P Le Bescop, P Adenot, F Bonville, P Jacquinet, JF Pineau, P & Felix, B 1996, 'Leaching of cement: study of the surface layer', *Cement and Concrete Research*, vol. 26, no. 11, pp. 1707-1715.
- Faucon, P Adenot, F Jorda, M & Cabrillac, R 1997, 'Behaviour of crystallised phases of Portland cement upon water attack', *Materials and Structures*, vol. 30, pp. 480-485.
- Faucon, P Adenot, F Jacquinet, JF Petit, JC Cabrillac, R & Jorda, M 1998, 'Long-term behaviour of cement pastes used for nuclear waste disposal: review of physico-chemical mechanisms of water degradation', *Cement and Concrete Research*, vol. 28, no. 6, pp. 847-857.
- Federal Highway Administration (FHWA) 1998, 'Corrosion Evaluation of Epoxy-coated, Metallic-clad and Solid Metallic Reinforcing Bars in Concrete', Report No. FHWA RD 98 153.
- Garrabrants, AC and Kosson, DS 2003, 'Modeling moisture transport from a Portland cement-based material during storage in reactive and inert atmospheres', *Drying Technology*, vol. 21, pp. 775-805.
- Garrabrants, A.C. Sanchez, F. et al. 2004, 'Changes in constituent equilibrium leaching and pore water characteristics of a Portland cement mortar as a result of carbonation' *Waste Management*, vol. 24, pp. 19-36.
- Garrabrants, AC and Kosson, DS 2005, 'Leaching processes and evaluation tests for inorganic constituents release from cement-based matrices' in *Solidification/ Stabilization of Hazardous, Radioactive and Mixed Wastes*, R Spence and C Shi (eds.), CRC Press (Boca Raton, USA), pp. 229-280.
- Gawin, D Pesavento, F Schrefler B.A. 2006, 'Hygro-thermo-chemo-mechanical modelling of concrete at early age and beyond. Part I: Hydration and hygro-thermal phenomena', *Int. J. Numer. Meth. Engng.*, vol. 67, pp. 299-331.
- Gervais, C. Garrabrants, A.C. Sanchez, F. and Kosson, D.S. 2004, 'The effects of carbonation and drying during intermittent leaching on the release of inorganic constituents from a cement-based matrix', *Cement and Concrete Research*, vol. 34, pp. 119-131.
- Ghods, P Chini, M Alizadeh, R & Hoseini, M 2005, 'The effect of different exposure conditions on the chloride diffusion into concrete in the Persian Gulf region', in *Proceedings of the ConMAT Conference*, N. Banthia et al. eds., Vancouver, Canada.
- Glass, GK & Buenfeld, NR 1997, 'Presentation of the chloride threshold level for corrosion of steel in concrete', *Corrosion Science*, vol. 39, pp. 1001-1013.
- Glasser, FP Kindness, A & Stronach, SA 1999, 'Stability and solubility relationships in AF<sub>m</sub> phases Part I. Chloride, sulfate and hydroxide', *Cement and Concrete Research*, vol. 29, pp. 861-866.

- Haga, K Sutou, S Hironaga, M Tanaka, S & Nagasaki, S 2005, 'Effects of porosity on leaching of Ca from hardened ordinary portland cement paste', *Cement and Concrete Research*, vol. 35, pp. 1764-1775.
- Hall, C 1994, 'Barrier performance on concrete: a review of fluid transport theory', *Materials and Structures*, vol. 27, pp. 291-306.
- Hansen, EJ & Saouma, VE 1999, 'Numerical simulation of reinforced concrete deterioration – part I: chloride diffusion', *ACI Materials Journal*, vol. 96, pp. 173-180.
- Harvie, CE Moller, N & Weare, JH 1984, 'The prediction of mineral solubilities in natural waters: The Na-K-Mg-Ca-H-Cl-OH-HCO<sub>3</sub>-CO<sub>3</sub>-CO<sub>2</sub>-H<sub>2</sub>O system to high ionic strengths at 25°C', *Geochimica et Cosmochimica Acta*, vol. 48, pp. 723-751.
- Hassanizadeh, M & Gray, WG 1979, 'General conservation equations for multi-phase systems: 1. Averaging procedure', *Advances in Water Resources*, vol. 2, pp. 131-144.
- Hausmann, DA 1967, 'Steel corrosion in concrete – How does it occur', *Materials Protection*, vol. 6, pp. 19-23.
- Heinz, D & Urbonas, L 2003, 'About thaumasite formation in Portland-limestone cement pastes and mortars – effect of heat treatment at 95°C and storage at 5°C', *Cement & Concrete Composites*, vol. 25, pp. 961-967.
- Helferich, F 1961, *Ion exchange*, McGraw-Hill, USA.
- Henocq, P Marchand, J Samson, E & Lavoie JA 2006, 'Modeling of ionic interactions at the C-S-H surface – Application to CsCl and LiCl solutions, in comparison with NaCl solutions, in *2nd Int. Symp. on Advances in Concrete through Science and Engineering (RILEM Proceedings 51)*, eds J. Marchand et al., RILEM Publications, France.
- Henocq, P Samson, E Marchand, J 2009, 'Chemical durability of cementitious materials: modeling the decalcification of hydrated C<sub>3</sub>S pastes', *in preparation*.
- Hidalgo, A De Vera, G Climent, MA Andrade, C & Alonso, C 2001, 'Measurements of chloride activity coefficients in real Portland cement paste pore solutions', *J. Am. Ceram. Soc.*, vol. 84, pp. 3008-3012.
- Hidalgo, A Petit, S Domingo, C Alonso, C & Andrade, C 2007, 'Microstructural characterization of leaching effects in cement pastes due to neutralisation of their alkaline nature – Part I: Portland cement pastes', *Cement and Concrete Research*, vol. 37, pp. 63-70.
- Higgins, DD 2003, 'Increased sulfate resistance of ggbs concrete in the presence of carbonate', *Cement & Concrete Composites*, vol. 25, pp. 913-919.
- Hill, J Byars, EA Sharp, JH Lynsdale, CJ Cripps, JC & Zhou, Q 2003, 'An experimental study of combined acid and sulfate attack of concrete', *Cement & Concrete Composites*, vol. 25, pp. 997-1003.
- Hinsenveld, M. 1992, 'A shrinking core model as a fundamental representation of leaching mechanism in cement stabilized waste', doctoral thesis, Department of Civil and Environmental Engineering, University of Cincinnati, Cincinnati, OH.

- Hobbs, DW & Taylor, MG 2000, 'Nature of the Thaumate sulfate attack mechanism in field concrete', *Cement and Concrete Research*, vol. 30, pp. 529-533.
- Hobbs, DW 2003, 'Thaumate sulfate attack in field and laboratory concretes: implications for specifications', *Cement & Concrete Composites*, vol. 25, pp. 1195-1202.
- Hong, SY & Glasser, FP 1999, 'Alkali binding in cement pastes Part I. The C-S-H phase', *Cement and Concrete Research*, vol. 29, pp. 1893-1903.
- Hope, BB Ip, AK & Manning, DG 1985, 'Corrosion and electrical impedance in concrete', *Cement and Concrete Research*, vol. 15, pp. 525-534.
- Hosokawa, Y Yamada, K Johannesson, BF & Nilsson, LO 2006, 'Models for chloride ion bindings in hardened cement paste using thermodynamic equilibrium calculations', in *2nd Int. Symp. on Advances in Concrete through Science and Engineering (RILEM Proceedings 51)*, eds J. Marchand et al., RILEM Publications, France.
- Houst, YF & Wittmann, FH 2002, 'Depth profiles of carbonates formed during natural carbonation', *Cement and Concrete Research*, vol. 32, pp. 1923-1930.
- Ishida, T Kawai, K & Sato, R 2006, 'Experimental study on decomposition processes of Friedel's salt due to carbonation', in *Proc. Int. RILEM-JCI Seminar on Concrete Durability (ConcreteLife '06)*, ed. K. Kovler, RILEM Publications, France, pp. 51-58.
- Johannesson, BF 2003, 'A theoretical model describing diffusion of a mixture of different types of ions in pore solution of concrete coupled to moisture transport', *Cement and Concrete Research*, vol. 33, pp. 481-488.
- Jones, MR Macphee, DE Chudek, JA Hunter, G Lannegrand, R Talero, R & Scrimgeour, SN 2003, 'Studies using  $^{27}\text{Al}$  MAS NMR of Aft and Aft phases and the Friedel's salt', *Cement and Concrete Research*, vol. 33, pp. 177-182.
- Juel, I Herfort, D Gollop, R Konnerup-Madsen, J Jakobsen, HJ & Skibsted, J 2003, 'A thermodynamic model for predicting the stability of thaumate', *Cement & Concrete Composites*, vol. 25, pp. 867-872.
- Kim, KH Jeon, SE Kim, JK & Yang, S 2003, 'An experimental study on thermal conductivity of concrete', *Cement and Concrete Research*, vol. 33, pp. 363-371.
- Kuhl, D Bangert, F & Meschke, G 2004, 'Coupled chemo-mechanical deterioration of cementitious materials. Part I: Modeling', *International Journal of Solids and Structures*, vol. 41, pp. 15-40.
- Kurtis, KE Monteiro, PJM & Madanat, S March-April 2000, 'Empirical models to predict concrete expansion caused by sulfate attack', *J. ACI Materials*, vol. 97, pp. 156-161. Errata published November-December 2000, V97 713.
- Lee, ST Moon, HY & Swamy, RN 2005, 'Sulfate attack and role of silica fume in resisting strength loss', *Cement & Concrete Composites*, vol. 27, pp. 65-76.
- Loudon N 2003, 'A review of the experience of thaumate sulfate attack by the UK Highways Agency', *Cement & Concrete Composites*, vol. 25, pp. 1051-1058.
- Luping, T & Nilsson, LO 1993, 'Chloride binding capacity and binding isotherms of OPC pastes and mortars', *Cement and Concrete Research*, vol. 23, pp. 247-253.

- Macphee, DE & Barnett, SJ 2004, 'Solution properties of solids in the ettringite-thaumasite solid solution series', *Cement and Concrete Research*, vol. 34, pp. 1591-1598.
- MacQuarrie, KTB & Mayer, KU 2005, 'Reactive transport modeling in fractured rock: a state-of-the-science review', *Earth-Science Reviews*, vol. 72, pp. 189-227.
- Mainguy, M Tognazzi, C Torrenti, JM & Adenot, F 2000, 'Modelling of leaching in pure cement paste and mortar', *Cement and Concrete Research*, vol. 30, pp. 83-90.
- Mainguy, M Coussy, O & Baroghel-Bouny, V 2001, 'Role of Air Pressure in Drying of Weakly Permeable Materials', *Journal of Engineering Mechanics*, vol. 127, pp. 582-592.
- Maltais, Y Samson, E & Marchand, J 2004, 'Predicting the durability of Portland cement systems in aggressive environments – laboratory validation', *Cement and Concrete Research*, vol. 34, pp. 1579-1589.
- Maltais, Y Marchand, J Henocq, P Zhang, T & Duchesne, J 2004b, 'Ionic interactions in cement-based materials: importance of physical and chemical interactions in presence of chloride or sulfate ions', in *Materials Science of Concrete VII*, ed. J.P. Skalny, American Ceramic Society, USA, pp. 181-208.
- Marchand, J Bentz, D Samson, E & Maltais, Y 2001, 'Influence of calcium hydroxide dissolution on the transport properties of hydrated cement systems', in *Materials Science of Concrete – Special Volume: Calcium Hydroxide in Concrete*, American Ceramic Society, USA, eds. J.P. Skalny et al., pp. 113-129.
- Marchand, J Samson, E Maltais, Y & Beaudoin, JJ 2002, 'Theoretical analysis of the effect of weak sodium sulfate solutions on the durability of concrete', *Cement & Concrete Composites*, vol. 24, pp. 317-329.
- Martín-Pérez, B Pantazopoulou, SJ & Thomas, MDA 2001, 'Numerical solution of mass transport equations in concrete structures', *Computers and Structures*, vol. 79, pp. 1251-1264.
- Masi, M Colella, D Radaelli, G & Bertolini, L 1997, 'Simulation of chloride penetration in cement-based materials', *Cement and Concrete Research*, vol. 27, pp. 1591-1601.
- Matschei, T Lothenbach, B Glasser, FP 2007, 'The AFm phase in Portland cement', *Cement and Concrete Research*, vol. 37, pp. 118-130.
- Mohammed, TU Hamada, H & Yamaji, T 2004, 'Concrete after 30 years of exposure – Part I: Mineralogy, microstructure and interfaces', *ACI Materials Journal*, vol. 101, pp. 3-12.
- Moranville, M Kamali, S & Guillon, E 2004, 'Physicochemical equilibria of cement-based materials in aggressive environments – experiment and modeling', *Cement and Concrete Research*, vol. 34, pp. 1569-1578.
- Mulenga, DM Stark, J & Nobst, P 2003, 'Thaumasite formation in concrete and mortars containing fly ash', *Cement & Concrete Composites*, vol. 24, pp. 907-912.
- Munshi, S & Boulfiza, M 2005, 'Chlorides ingress and carbonation: effect on partitioning between free and bound chlorides', *Proceedings of the ConMAT Conference*, Vancouver Canada.
- Nagesh, M & Bhattacharjee, B 1998, 'Modeling of chloride diffusion in concrete and determination of diffusion coefficients', *ACI Materials Journal*, vol. 95, pp. 113-120.
- Naik, NN Jupe, AC Stock, SR Wilkinson, AP Lee, PL & Kurtis, KE 2006, 'Sulfate attack monitored by microCT and EDXRD: Influence of cement type, water-to-cement ratio, and aggregate', *Cement and Concrete Research*, vol. 36, pp. 144-159.

- Nielsen, EP Herfort, D Geiker, MR 2005, 'Binding of chloride and alkalis in portland cement systems', *Cement and Concrete Research*, vol. 35, pp. 117-123.
- Nobst, P & Stark, J 2003, 'Investigations on the influence of cement type on thaumasite formation', *Cement & Concrete Composites*, vol. 25, pp. 899-906.
- Odler, I & Colan-Subauste, J 1999, 'Investigations on cement expansion associated with ettringite formation', *Cement and Concrete Research*, vol. 29, pp. 731-735.
- Ouyang, C Nanni, A & Chang, WF 1988, 'Internal and external sources of sulfate ions in portland cement mortar: two types of chemical attack', *Cement and Concrete Research*, vol. 18, pp. 699-709.
- Pajares, I Martinez-Ramirez, S & Blanco-Varela, MT 2003, 'Evolution of ettringite in presence of carbonate, and silicate ions', *Cement & Concrete Composites*, vol. 25, pp. 861-865.
- Pankow, JF 1994, *Aquatic Chemistry Concepts*, Lewis Publishers, USA.
- Papadakis, VG Vayenas, CG & Fardis, MN 1991, 'Fundamental modeling and experimental investigation of concrete carbonation', *ACI Materials Journal*, vol. 88, pp. 363-373.
- Planel, D Sercombe, J Le Bescop, P Adenot, F & Torrenti, J-M 2006, 'Long-term performance of cement paste during combined calcium leaching-sulfate attack: kinetics and size effect', *Cement and Concrete Research*, vol. 36, pp. 137-143.
- Plummer, LN Busenberg, E 1982, 'The solubilities of calcite, aragonite and vaterite in CO<sub>2</sub>-H<sub>2</sub>O solutions between 0 and 90°C, and an evaluation of the aqueous model for the system CaCO<sub>3</sub>-CO<sub>2</sub>', *Geochimica et Cosmochimica Acta*, vol. 46, pp. 1011-1040.
- Reardon, EJ 1990, 'An ion interaction model for the determination of chemical equilibria in cement/water systems', *Cement and Concrete Research*, vol. 20, pp. 175-192.
- Reardon, EJ 1992, 'Problems and approaches to the prediction of the prediction of the chemical composition in cement/water systems', *Waste Management*, vol. 12, pp. 221-239.
- Rémond, S Bentz, DP & Pimienta, P 2002, 'Effects of the incorporation of Municipal Solid Waste Incineration fly ash in cement pastes and mortars – II: Modeling', *Cement and Concrete Research*, vol. 32, pp. 565-576.
- Rigo da Silva, CA, Reis, RJP Lameiras, FS & Vasconcelos, WL 2002, 'Carbonation-related microstructural changes in long-term durability concrete', *Materials Research*, vol. 5, pp. 287-293.
- Romer, M Holzer, L & Pfiffner, M 2003, 'Swiss tunnel structures: concrete damage by formation of thaumasite', *Cement & Concrete Composites*, vol. 25, pp. 1111-1117.
- Saetta, A Scotta, R & Vitaliani, R 1993, 'Analysis of chloride diffusion into partially saturated concrete', *ACI Materials Journal*, vol. 90, pp. 441-451.
- Saetta, A Schrefler, BA & Vitaliani, R 1993, 'The carbonation of concrete and the mechanism of moisture, heat and carbon dioxide flow through porous materials', *Cement and Concrete Research*, vol. 23, pp. 761-772.
- Saetta, AV & Vitaliani, RV 2004, 'Experimental investigation and numerical modeling of carbonation process in reinforced concrete structures Part I: Theoretical formulation', *Cement and Concrete Research*, vol. 34, pp. 571-579.

- Saito, H & Deguchi, A 2000, 'Leaching tests on different mortars using accelerated electrochemical method', *Cement and Concrete Research*, vol. 30, pp. 1815-1825.
- Samson, E Marchand, J Snyder, KA & Beaudoin, JJ 2005, 'Modeling ion and fluid transport in unsaturated cement systems in isothermal conditions', *Cement and Concrete Research*, vol. 35, pp. 141-153.
- Samson, E & Marchand, J 2006, 'Multiionic approaches to model chloride binding in cementitious materials', in *2nd Int. Symp. on Advances in Concrete through Science and Engineering (RILEM Proceedings 51)*, eds J. Marchand et al., RILEM Publications, France.
- Samson, E & Marchand, J 2007, 'Modeling the effect of temperature on ionic transport in cementitious materials', *Cement and Concrete Research*, vol. 37, pp. 455-468.
- Sanchez, F 1996, 'Étude de la lixiviation de milieux poreux contenant des espèces soluble: Application au cas des déchets solidifiés par liants hydrauliques' doctoral thesis, Institut National des Science Appliquées, Lyon, France, 269 pp.
- Sanchez, F Gervais, C et al. 2002, 'Leaching of inorganic contaminants from cement-based waste materials as a result of carbonation during intermittent wetting' *Waste Management*, vol. 22, pp. 249-260.
- Santhanam, M Cohen, MD & Olek, J 2001, 'Sulfate attack research', *Cement and Concrete Research*, vol. 31, pp. 845-851.
- Schrefler, BA 2004, 'Multiphase flow in deforming porous material', *International Journal for Numerical Methods in Engineering*, vol. 60, pp. 27-50.
- Selih, J Sousa, ACM & Bremner, TW 1996, 'Moisture transport in initially fully saturated concrete during drying', *Transport in porous media*, vol. 24, pp. 81-106.
- Sibbick, T Fenn, D & Crammond, N 2003, 'The occurrence of thaumasite as a product of seawater attack', *Cement & Concrete Composites*, vol. 25, pp. 1059-1066.
- Simunek, J & Suarez, DL 1994, 'Two-dimensional transport model for variably saturated porous media with major ion chemistry', *Water Resour. Res.*, vol. 30, pp. 1115-1133.
- Skalny, J Marchand, J & Odler, I 2002, *Sulfate Attack on Concrete*, Spon Press, New-York.
- Song, HW Kwon, SJ Byun, KJ & Park, CK 2006, 'Predicting carbonation in early-aged cracked concrete', *Cement and Concrete Research*, vol. 36, pp. 979-989.
- Sten-Knudsen, O 2002, *Biological Membranes – Theory of transport, potentials and electric impulses*, Cambridge University Press, UK.
- Suryavanshi, AK Scantlebury, JD & Lyon, SB 1995, 'The binding of chloride ions by sulphate resistant Portland cement', *Cement and Concrete Research*, vol. 25, pp. 581-592.
- Suryavanshi, AK Scantlebury, JD & Lyon, SB 1996, 'Mechanism of Friedel's salt formation in cement rich in tri-calcium aluminate', *Cement and Concrete Research*, vol. 26, pp. 717-72.
- Swaddiwudhipong, S Wong, SF Wee, TH & Lee, SL 2000, 'Chloride ingress in partially and fully saturated concrete structures', *Concrete Science and Engineering*, vol. 2, pp. 17-31.
- Tang, L & Nilsson, LO 1993, 'Chloride binding capacity and binding isotherms of OPC pastes and mortars', *Cement and Concrete Research*, vol. 23, pp. 247-253.
- Taylor, HFW 1997, *Cement Chemistry*, Thomas Telford, London.

- Thomas, MDA 1999, 'Modeling chloride diffusion in concrete – Effect of fly ash and slag', *Cement and Concrete Research*, vol. 29, pp. 487-495.
- Tian, B & Cohen, MD 2000, 'Does gypsum formation during sulfate attack on concrete lead to expansion?', *Cement and Concrete Research*, vol. 30, pp. 117-123.
- Truc, O Ollivier, JP & Nilsson, LO 2000, 'Numerical simulation of multi-species diffusion', *Materials and Structures*, vol. 33, pp. 566-573.
- Tsivilis, S Kakali, G Skaropoulou, A Sharp, JH & Swamy, RN 2003, 'Use of mineral admixtures to prevent thaumasite formation in limestone cement mortar', *Cement & Concrete Composite*, vol. 25, pp. 969-976.
- Tuutti, K 1982, 'Corrosion of steel in concrete', *Swedish Cement and Concrete Research Institute*, Report Fo 4:82. CBI. Stockholm. Sweden.
- van Gerven, T Cornelis, G Vandoren, E Garrabrants, AC Sanchez, F Kosson, DS and Vandecasteele, C 2006, 'Effects of progressive carbonation on heavy metal leaching from cement-bound waste', *AIChE Journal* vol. 52, pp. 826-837.
- van Gerven, T Cornelis, G et al. 2007, 'Effects of carbonation and leaching on porosity in cement-bound waste', *Waste Management*, vol. 27, pp. 977-985.
- West, RE & Hime, WG 1985, 'Chloride profiles in salty concrete', *Materials Performance*, vol. 24, pp. 29-36.
- West, RE & Hime, WG 1985, 'Chloride profiles in salty concrete', *Materials Performance*, vol. 24, pp. 29-36.
- Whitaker, S 1998, 'Coupled transport in multiphase systems: a theory of drying', in *Advance in Heat Transfer 31*, J.P. Hartnett et al. eds., pp. 1-104.
- Xi, Y Bazant, ZP Molina, L & Jennings, HM 1994, 'Moisture diffusion in cementitious materials - Moisture capacity and diffusivity', *Advanced Cement Based Materials*, vol. 1, pp. 258-266.
- Xu, T Apps, JA & Pruess, K 2004, 'Numerical simulation of CO<sub>2</sub> disposal by mineral trapping in deep aquifers', *Applied Geochemistry*, vol. 19, pp. 917-936.
- Xu, T Sonnenthal, E Spycher, N & Pruess, K 2006, 'TOUGHREACT - a simulation program for non-isothermal multiphase reactive geochemical transport in variably saturated geologic media: applications to geothermal injectivity and CO<sub>2</sub> geological sequestration', *Computers & Geosciences*, vol. 32, pp. 145-165.
- Yokozeki, K Watanabe, K Sakata, N & Otsuki, N 2004, 'Modeling of leaching from cementitious materials used in underground environment', *Applied Clay Science*, vol. 26, pp. 293-308.
- Zalc, JM Reyes, SC & Iglesia, E 2004, 'The effects of diffusion mechanism and void structure on transport rates and tortuosity factors in complex porous structures', *Chem. Eng. Sci.*, vol. 59, pp. 2947-2960.
- Zemaitis, JF Clark, DM & Rafal, M 1986, 'Scrivner N.C., Handbook of aqueous electrolyte thermodynamics', *American Institute of Chemical Engineers*, New-York, USA.
- Zhou, Q Hill, J Byars, EA Cripps, JC Lynsdale, CJ & Sharp, JH 2006, 'The role of pH in thaumasite sulfate attack', *Cement and Concrete Research*, vol. 36, pp. 160-170.





U.S. DEPARTMENT OF  
**ENERGY**



**SRNL**  
SAVANNAH RIVER NATIONAL LABORATORY



**CRES P**



**VANDERBILT  
UNIVERSITY**



UNITED STATES NUCLEAR REGULATORY COMMISSION

**NIST**  
National Institute of  
Standards and Technology



**ECN**



**SIMCO**  
Technologies inc.